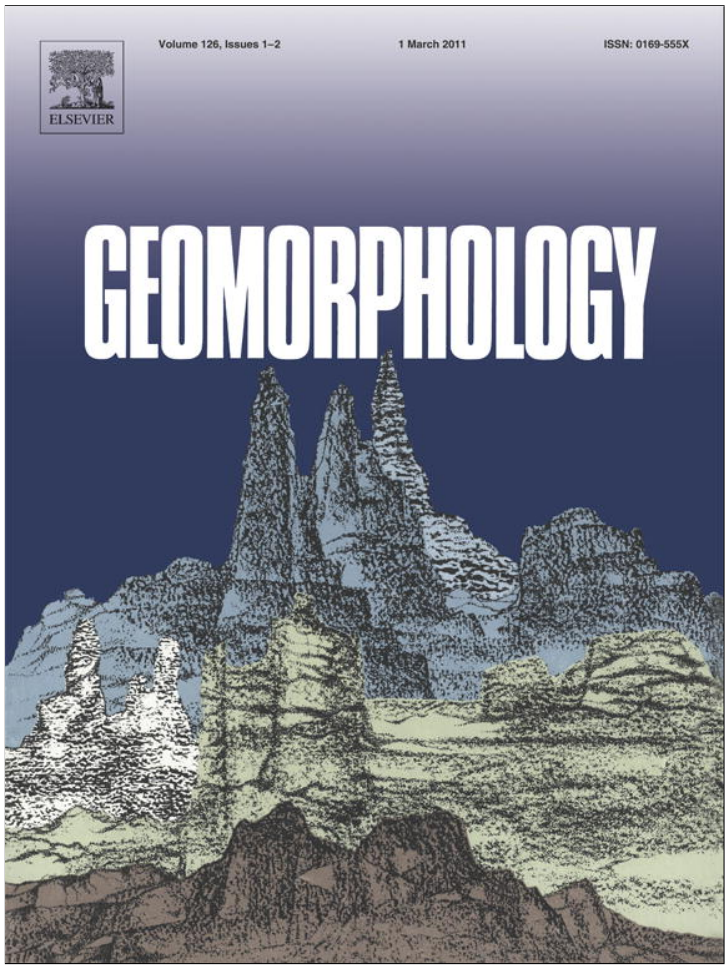

Geomorphology 126 (2011) 201–216

Contents lists available at ScienceDirect

Geomorphology

journal homepage: www.elsevier.com/locate/geomorph

Dynamics of a nearshore bar system in the northern Adriatic: A video-based morphological classification

Clara Armaroli [1], Paolo Ciavola *

Dipartimento di Scienze della Terra, Università di Ferrara, Via Saragat 1, 44100 Ferrara, Italy

ARTICLE INFO

Article history:
Received 2 April 2010
Received in revised form 29 October 2010
Accepted 10 November 2010
Available online 23 November 2010

Keywords:
Nearshore bars
Coastal morphodynamics
Video-monitoring
Microtidal beaches
Intermediate beach states

ABSTRACT

The aim of this paper is to define a simplified morphodynamic classification suitable for low energy beaches exposed to microtidal conditions. The study site is located in the northern Adriatic (in Italy), it is an almost 2 km-long rectilinear beach bordered at the northern edge by coastal structures and at the southern end by a small river inlet. The mechanisms related to the evolution of the submerged part of the beach were derived from video-monitoring using Argus technology. The morphodynamic evolution of the system was studied using an automatic procedure on images for the characterisation of nearshore bars that showed good correspondence with hand-based (visual) interpretation. To apply this automatic procedure, the bar's plan crest shape was mapped using cross-shore pixel luminosity transects traced on time-averaged video images. A careful sensitivity analysis was undertaken to determine the best spacing between transects for the correct tracing of the shape of the bar crest. The error associated to a transect spacing every 25 m resulted in being comparable with the pixel resolution in the area and with the error found comparing the video interpretation with bathymetric surveys.
From the study of a four and a half year dataset (February 2003–May 2007), the submerged beach was found to be characterised by the presence of a single bar in the area next to coastal protection structures. However, moving southwards of these, inner and outer bars were present. The morphodynamics of the outer bar and its plan shape modifications were dominated by rhythmic forms. Occasionally, after high energy events, the bar became rectilinear but during the following lower energy periods rhythmicity was re-established, supporting the hypothesis of self-organization mechanisms. The cross-shore position of the bar's crests only showed limited cross-shore mobility through time.

1. Introduction

One of the main questions that have fascinated geologists and oceanographers specialising in coastal studies is stated at the beginning of one of the first quantitative studies on the subject (Huntley and Bowen, 1975): "Why are some beaches steep and other shallow?" Obviously the morphology results as a combination of factors such as the grain size of beach material and beach slope, which in turn is dependent on exposure to wave action. This explains why changes in wave climate can modify beach slope at time intervals of the order of hours to days and often produce cyclic changes of beach profile over longer time scales. At the time of the study of Huntley and Bowen (1975), laboratory modelling was largely empirical and the relevance of 2-D laboratory experiments to field conditions was doubtful. Therefore the authors focused their attention mainly on hydrodynamic processes such as wave breaking, energy dissipation, swash oscillations and presence of edge waves, which were believed to be a driving factor for the formation of rhythmic features (Bowen and Inman, 1971).

About 10 years later, with the publication of the seminal work of Wright and Short (1984) on beach morphodynamics, coastal research adopted a new approach to the study of beaches, wherefore physical measurements and monitoring of morphological changes became closely linked, providing input to energy descriptors (e.g. surf scaling and surf similarity parameters) that account for the relationship between beach slope and the type of breakers. The paper cited above was in reality a comprehensive review of a large field database collected by the authors in the period 1976–1982 (see also Short, 1979; Wright et al., 1979, 1982a, 1982b; Wright and Short, 1983), with study sites spanning from micro- to macro-tidal conditions, whereby wave energy (modal breaking wave height) varied from low (0.3 m) to high (5 m). Recently Short (2006) reviewed over 10,000 beach systems all-around the coast of Australia and basically showed that such a wide scale generalization is still of utmost importance for beach classifications. The applicability of the classification has been widely validated by studies carried out in various parts of the world, including the Mediterranean (e.g. Gómez-Pujol et al., 2007). However, in such a context dominated by an average low wave energy, the

* Corresponding author. Tel.: +39 0532974622; fax: +39 0532974767.
E-mail addresses: rmrclr@unife.it (C. Armaroli), cvp@unife.it (P. Ciavola).
[1] Tel.: +39 0532974739; fax: +39 0532974767.

0169-555X/$ – see front matter © 2010 Elsevier B.V. All rights reserved.
doi:10.1016/j.geomorph.2010.11.004

calculation of morphodynamic indexes based on modal wave energy alone may be misleading, as the duration of high energy events may play an important role in controlling dominant beach states (Armaroli et al., 2007; Jiménez et al., 2008).

Field studies of bar morphodynamics in the Mediterranean are scarce and particularly limited regarding rhythmic systems. Noticeable contributions are those of Barusseau and Saint-Guily (1981), Goldsmith et al. (1982), Bowman and Goldsmith (1983), Guillén and Palanques (1993), Certain (2002) and Certain and Barusseau (2005). The studies of beaches in the Mediterranean using Argus technology are so far rare and only focussed on the shoreline variability of beaches protected by structures (e.g. Armaroli et al., 2006b; Ojeda and Guillén, 2006, 2008; Ojeda et al., 2006; Archetti, 2009). To the knowledge of the authors, most previous studies of bar morphodynamics along open coastlines in the Mediterranean have not used high frequency monitoring methods based on video monitoring, as the studies cited above reach their conclusions on the basis of traditional echo-sounding surveys. The only published work on nearshore bar variability using Argus video methods (Holman and Stanley, 2007) is that of Ribas et al. (2010) who proved the suitability of the technique for studying tideless beaches adjacent to coastal structures along the urban coast of Barcelona.

As traditional surveys (e.g. bathymetric surveys and aerial photography) cannot resolve short-term (from hours to days) large-scale bed changes, the response of such systems to varying wave energy changes during and immediately after storms is not known. In addition to financial restrictions to be able to carry out frequent bathymetric surveys, logistical limitations exist (e.g. rough seas for soundings by boat, water turbidity for LIDAR flights) and normally fair-weather conditions are preferred.

As Turner et al. (2006) observed, the use of video systems in the last 20 years has allowed the monitoring of coastal changes at a frequency (from minutes to hours) which is unthinkable for direct bathymetric surveys (from days to months). Recent applications of video monitoring have enhanced the understanding of the evolution of large-scale morphologies on open coasts (e.g. Ortega-Sánchez et al., 2008), coastal spits (e.g. Medellín et al., 2008) and inlets (e.g. Siegle et al., 2007). Morphological numerical modelling of nearshore bar evolution has been enhanced by the coupling with video systems (e.g. Coco et al., 2004; Ranasinghe et al., 2004). However, as remarked by Stive and Reniers (2003), the non-linearity of surf zone processes is testified by the complexity associated with bar morphodynamics and with beach-cusps, which at present cannot be fully explained without citing the debate between self-organization and forced response.

The general scope of the current paper was to analyze the morphodynamic behaviour of an intermediate beach in the Mediterranean, focusing on changes in the plan shape of the nearshore bar and developing a morphodynamic classification able to account for spatial variability of the bar crest at scales of hundreds of meters alongshore. Since according to the reference work cited above these changes may be ephemeral and only seen during or immediately after high energy events, traditional surveying methods (e.g. bathymetries) may not be the appropriate mode of study because of the difficulty of accessing the surf-zone in these conditions. On the other hand, remote-sensing techniques based on video-monitoring allow a continuous observation of the breaking wave patterns which are related to the submerged morphologies. Thus, the study was focused on the development of a semi-quantitative morphodynamic classification, based on the observation of breaking wave patterns.

1.1. Field site

Lido di Dante is a small village in the Emilia–Romagna Region (northern Italy), 10 km from the city of Ravenna (Fig. 1). The beach is a 3 km-long stretch of coast, almost aligned in a N–S direction, divided in two parts: the one in front of the Lido di Dante village (almost 1 km) is protected by a breakwater and three groynes. The other one (almost 2 km) is completely natural with dunes backed by a pine forest (Fig. 1). The present study deals with the unprotected part of the beach that extends from the southernmost groyne of the protected beach to the Bevano River mouth (Fig. 1).

According to Ciavola et al. (2003), the shoreline started to retreat in the late 1970 s, initially because of a regional decrease in river sediment supply and subsidence generated by gas extraction (Teatini et al., 2005). The comparison between several HWLs (High Water Lines, *cf.* Dolan and Hayden, 1983) mapped on aerial photos, using GIS techniques, reveals that the area still suffers from erosion even though many coastal protection schemes were undertaken to avoid the loss of sediment and the narrowing of the beach. The coastal structures in front of the village were built starting from the 1980s (Casadei et al., 1998). Three rock groynes and a breakwater were constructed and sandbags were placed on the beach. Moreover, several replenishments were undertaken with either sands extracted from inland quarries or dredging relict marine sediments accumulated in front of the Emilia–Romagna coast. In April–May 2007 a beach replenishment was undertaken, placing 107,000 m^3 of sand (M. Ceroni, personal communication) both inside the protected area and on the northern part of the natural beach, up to 800 m southwards from the groyne. Despite all these interventions the erosion is still undergoing and the beach is narrowing, mainly in the natural area next to structures. The southern boundary of the study area is delimited by a river mouth (Bevano River). Between 2003 and 2006 the river outlet was very active and moved northward by several hundreds of meters, eroding the dunes laterally (Balouin et al., 2006a). To prevent the erosion, the Regional Authorities moved the mouth 500 m southwards opening a new outlet and reconstructing the dunes (Gardelli et al., 2007).

The tidal regime is strongly asymmetric, showing both diurnal and semi-diurnal components. The maximum tidal range is about 0.9–1 m during spring tides. The wave climate is usually of low energy, with $0.5 \leq H_s < 1$ m, mainly from the east (65% of occurrences) (Gambolati et al., 1998). The 11% of data is defined as calm conditions ($H_s < 0.5$ m), therefore the total occurrence of low energy conditions is 76% (Idroser, 1996). Two different storm directions prevail in the northern Adriatic Sea: the Scirocco, from SE, and the Bora from E-NE. A high energy event ($H_s > 3$ m) occurred at the beginning of 2003 but unfortunately the Argus station was not operative yet. For further details on the characteristics of the events during the monitored period see Armaroli et al. (2007). The studied period was characterised by variable wave conditions (Fig. 2) and included a very strong storm which occurred in September 2004 with a wave height of more than 5 m, equivalent to a 25-year return period event (Ciavola et al., 2007). Energetic events occurred at the end of 2004, and at the beginning of 2005 and 2006. These last two periods were characterised by the clustering of several storms. From Spring 2006 to the end of 2007, the wave height did not exceed 3 m and was most of the time below 2 m (Fig. 2).

The sub-aerial beach sediment mean size is between fine to medium sand (2.3–1.1 φ); the submerged beach is composed of fine sand (2.22 φ; Gardelli et al., 2007). The submerged beach, with depths below Low Water Springs (−0.5 below MSL), in the area is characterised by the presence of offshore bars (Armaroli et al., 2007). The bathymetry close to the groyne shows a single bar next to the shoreline. Moving to the south, the bathymetry changes and the system is composed of two bars: the outer one is the termination of the single bar located near the groyne and its cross-shore distance from the shore increases along the study zone; the inner one is alternately attached and detached from the shore and shows rhythmic forms (Fig. 3). The morphodynamics of the submerged features are characterised by different states that change frequently according to variability in wave energy levels, but once they reach an equilibrium configuration they are stable over long periods (Armaroli et al., 2007).

As described by Armaroli et al. (2005) and Balouin et al. (2006b), the study area can be divided in three main parts. The northern one is characterised by shoreline and dune foot retreat, one bar attached/

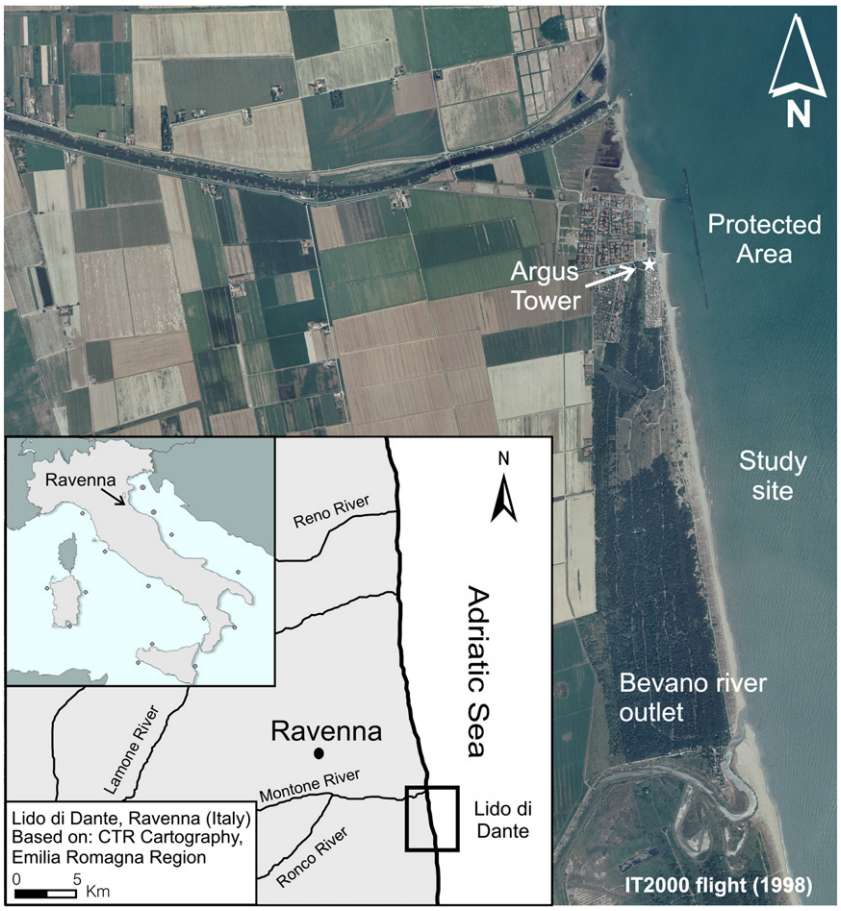

Fig. 1. Lido di Dante (Ravenna) map location and aerial photograph (IT2000 flight, Regione Emilia Romagna).

detached to the shoreline, complex wave breaking patterns on timex images, and the prevalence of rhythmic forms. The central one has shoreline oscillations (longshore movement of intertidal forms, see Kroon et al., 2007), an oscillating/eroding dune foot, and a submerged beach where the single offshore bar in the northern area splits into two bars (Fig. 4). One bar is parallel to the shoreline (attached and detached) and connected to the Bevano River mouth, the other one is oriented at an angle, its cross-shore distance from the shoreline increasing southward, and attached to the Bevano River submerged delta. To notice that the river location indicated in Fig. 1 is the position it had in 1998. River engineering works moved it 500 m southwards in March 2006 (Gardelli et al., 2007). The southern area is characterised by a stable shoreline, healthy dunes and two bars (as for the central part).

1.2. The Argus system at Lido di Dante

This third generation Argus system (Holman and Stanley, 2007) was installed on an observation tower in February 2003 located in the southern part of Lido di Dante (Fig. 1) for the Coastview Project (Davidson et al., 2007). It consists of four cameras, three looking at the protected part of the beach and one looking at the natural one. The present paper will only focus on data collected by the camera that monitors the natural area. The coordinate system has its origin centred on the Argus tower, the x-axis perpendicular to the shoreline (cross-shore) and the y-axis parallel to the coast (longshore). The positive directions are respectively to the east and to the north. The axes are slightly rotated with respect to the N–S direction by −9.8°. This rotation was imposed in order to locate the y-axis exactly parallel to the breakwater. The standard Argus video products captured by the system are snapshot, timex, variance and day-timex (Holman and Stanley, 2007). Camera 1 (hereafter referred as C1), the one looking at the natural part of the beach, captures the images at the beginning of every hour, during daylight. Each camera works independently and separately from the others. When one camera is working, the others are switched off. The C1 resolution is very good in the cross-shore direction: between 0.1 m to 4 m up to 1700 m southward of the camera. The longshore resolution is worse: it decreases from 4 m to 30 m moving away from the coordinate system's origin.

Hourly timex images are the products used in this paper to classify the submerged beach because, when waves are breaking, it is possible to see the shape and position of the bars below MSL (for further details see Lippmann and Holman, 1990; Holland et al., 1997). It is important to note that the two bar systems are typically visible on the images, one next to the shoreline and one offshore. This paper only analyses and describes the outer bar. The morphological setting of the nearshore makes it difficult to study the inner and the outer bar at the same time. The inner bar is attached to the shoreline and can be found within the intertidal beach profile. The best conditions to see the crest of the nearshore bar on the Argus images are under moderate waves up to 1.5 m high, which break a second time close to the shoreline in a typically chaotic and wide breaking zone. Under these conditions the inner bar cannot be discriminated. The other limitation is the resolution of the camera in the far field of view, which cannot resolve small features which are normally present in the central and southern portion of the images (e.g. swash bars).

2. Methods

2.1. The identification of the bar on the images

To produce a morphodynamic classification of the submerged beach, the Argus timex images were initially selected for their best quality to

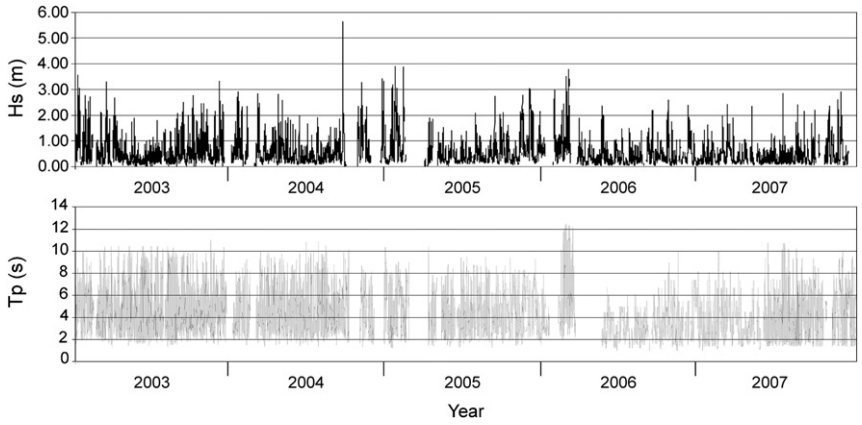

Fig. 2. Wave height (H_s, upper panel) and period (T_p, lower panel) values from 2003 to 2007.

classify the bar and to extract the position and plan shape of its crest. Two different types of analyses were performed. First, a qualitative visual morphodynamic classification took place using timex plan views. Second, the extraction of the position of the bar trough sampling of the pixel luminosity intensity was done along equally spaced cross-shore arrays. Each one of the above methodologies is described below in detail. The analysis includes the period between February 2003 (installation of the Argus system) and April 2007. In May 2007 a replenishment was undertaken in the northern part of the study area, generating a significant perturbation to the submerged and emerged beach system that cannot be compared to the previous period.

Before starting the analysis, it was important to define the optimal hydrodynamic conditions to see the submerged bars on timex images and what was the positional error associated to the resulting bar plan crest if compared to direct surveys. According to Armaroli et al. (2006a), the best hydrodynamic conditions to see the bars at this site are a low tide elevation between 0 m and −0.20 m below MSL and an offshore wave height (H_{rms}) lower or equal to 1.5 m. For tidal levels different from those, either the breaking occurs directly on the shoreline (higher tide levels) or the surf zone becomes too wide and the breaking point

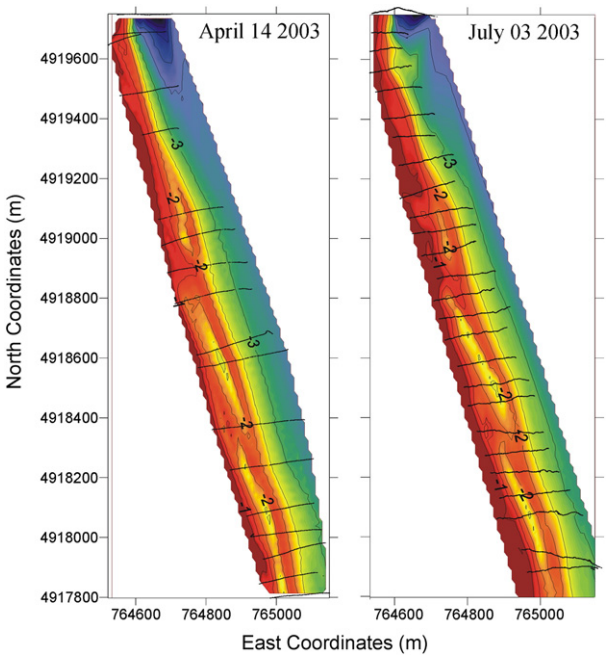

Fig. 3. Comparison between single-beam echosounder surveys performed in April 2003 (left figure) and July 2003 (right figure). Notice the persistence of crescentic bars. Coordinates in UTM32, datum ED50.

undefined. For wave heights lower than the threshold, waves do not break over the bar. For higher waves, breaking occurs seaward of the bar's crest and again the surf zone becomes too wide.

Van Enckevort and Ruessink (2001) found that the luminosity maximum is better associated, if compared to the bathymetry, with the position of the maximum cross-shore perturbation with respect to a barless underlying profile. This was obtained through the comparison between an average profile without the bar (using a time series of cross-shore bathymetric profiles for 34 years at Egmond aan Zee, The Netherlands) and the profile with the bar. They concluded that Argus video intensities reflect the maximum perturbation rather than the minimum depth. In a recent paper by Ribas et al. (2010) an alternative approach was used, as the authors did not have access to long-term bathymetric measurements. As they were dealing with terraced beach profiles, they defined the bar location as the position of the terrace edge or the maximum slope change in the profile. This alternative method could be applied to the inner bar of our study site, typically with a Low Tide Terrace. However, for the offshore bar we preferred to use a site-specific definition as explained below.

For the Lido di Dante site, the bar crest in direct surveys was defined as the minimum depth between the trough and the bar's seaward foot. In this case insufficient background information was available to reconstruct a reference profile and to find the location of the maximum perturbation. Thus, it was decided to consider the minimum depth of the bedform as the bar crest. The error associated to the comparison between Argus intensities and the minimum depth on direct surveys will be discussed later in detail.

Alexander and Holman (2004) say that although wave breaking always results in an increase in the cross-shore intensity profile, variations in the relative intensity values over multiple bars and the shore break at the same alongshore location, and morphological variability in the profile make the use of intensity maxima to identify sand bars unreliable, unless the accuracy is properly tested against measurements. The error was investigated by comparison of the planar position of the bar extracted from timex images with the morphology surveyed during a bathymetric LIDAR flight performed by ENI (Ente Nazionale Idrocarburi) in early June 2006.

2.2. The morphodynamic visual classification

The first classification of single bar morphologies was that of Wright and Short (1984), which relates the presence of the bar with values of dimensionless fall velocity (Dean, 1973) exceeding 1. Wright and Short did not examine in detail the topic of longshore variability and the role of infragravity motions, as it was later done by Lippmann and Holman (1990). The advancement in understanding provided by these authors compared to the first one is explained with the technology used for the studies. Wright and Short (1984) used traditional beach surveys, thus

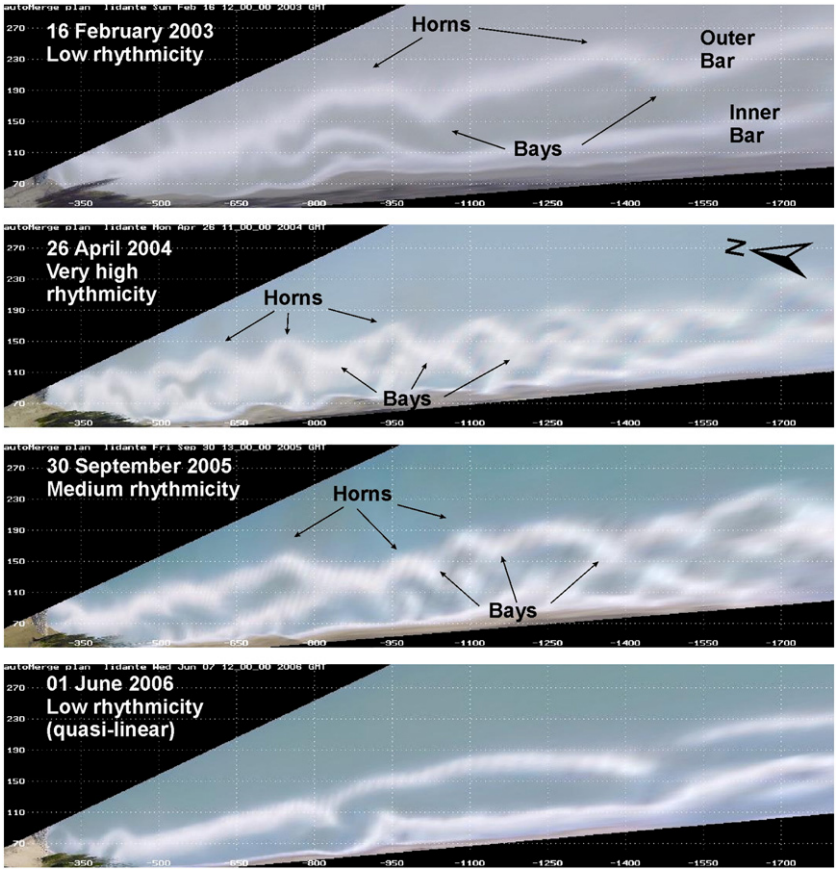

Fig. 4. Four examples of plan views showing different bar configurations (low, medium, high and very high rhythmicity). Horns and bays of rhythmic bars are indicated.

limited in temporal and spatial coverage, while Lippmann and Holman (1990) applied for the first time video-monitoring. Both groups of authors did not deal with multiple bar formation and characteristics, as this was later done by Short and Aagaard (1993) who suggested the relationship between nearshore geometry and incident wave period. According to them, this in turn limits the number of IG (Infra-Gravity) nodes and anti-nodes that can be accommodated inside the surf zone.

In comparison, video-monitoring provides large databases that can be interpreted by experienced users. Image interpretation is strongly dependent on the individual's opinion, depending on his/her skill or on image quality (e.g. colour saturation and contrast). The subjectivity of such an approach is possibly the bigger obstacle for visually-based procedures. Previous work based on visual examination of images found that often there is a good agreement between different interpreters (Lippmann and Holman, 1990; Armaroli et al., 2006a) but the main limitation of the procedure is the time-consuming effort to produce results. The time spent following this procedure increases together with the complexity of the study site. In the process of thinking of how to classify the bars at Lido di Dante, we decided to concentrate on the longshore uniformity in position and shape of the bar crest, basically merging the conceptual approach of Wright and Short (1984) with that of Lippmann and Holman (1990).

The morphodynamic classification of the submerged beach was performed through the observation of the plan shape of the bars, as marked by breaking waves on timex images. The classification proposed in this paper neither deals with the absolute position (longshore and cross-shore) of the bar crest nor with the relationship between the outer and the inner bar or with the shoreline, but only with its "shape". This last term identifies the number of rhythmic features composing the bar. The terminology used to create the classification relates to the presence or absence of 3-D forms. In Table 1 all the acronyms used for each morphological class are listed, together with their correspondence to the bar plan-shape. The sequence of each acronym follows a north–south direction (Fig. 5). The acronyms used include R for rhythmic/very rhythmic forms, L for linear and Ob(L) for oblique and linear ones. The last definition is related to the formation of oblique bars (increasing

Table 1
Predominant bar plan shapes and correspondent acronyms used for the visual classification.

Bar plan shape	Characteristics	Acronym
Linear	Straight bar crest parallel to the shoreline	L
Rhythmic (1 to 2 three-dimensional forms)	Crescentic bars with up to two waveforms	R
Rhythmic (>2 three-dimensional forms)	Crescentic bars with more than two waveforms	RR
Oblique – Southern area only	Straight bar crest, not continuous and at an angle with the shoreline	Ob
Oblique (almost linear) – Southern area only	Straight bar crest, not continuous, at an angle with the shoreline and becoming linear moving away from the observation point	Ob(L)
Linear and rhythmic [and *vice versa*]	Straight bar crest, parallel to the shoreline and becoming rhythmic moving away from the observation point. Up to two waveforms visible	L(R) [R(L)]
Linear and very rhythmic [and *vice versa*]	Straight bar crest, parallel to the shoreline and becoming rhythmic moving away from the observation point. More than two waveforms visible	L(RR) [RR(L)]

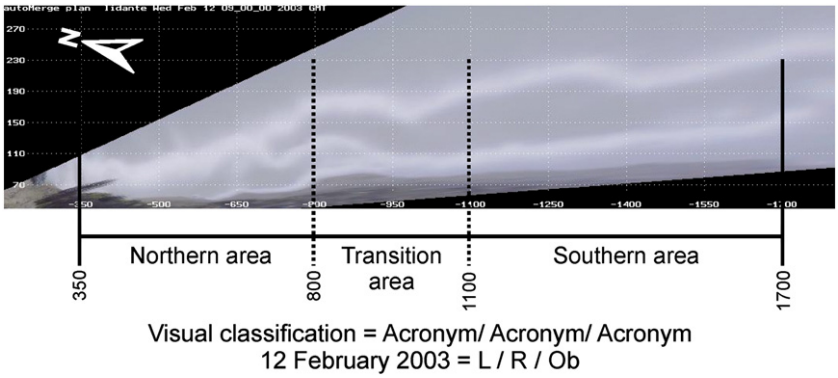

Fig. 5. Plan view of 12th February 2003 and scheme of the visual classification. Example of 12th February 2003 classification. The abbreviations L, R and Ob respectively indicate Linear, Rhythmic and Oblique bars.

distance of the bar from the shoreline) that are linear along most of their length and therefore cannot be considered as proper crescentic forms even if they are attached together at one end (Fig. 5). These types of morphologies are not unusual in the Mediterranean, as they were reported by Certain and Barusseau (2005) at Lido de Sete, on the Languedoc French coast. In this case the authors call them "sinuous" bars,

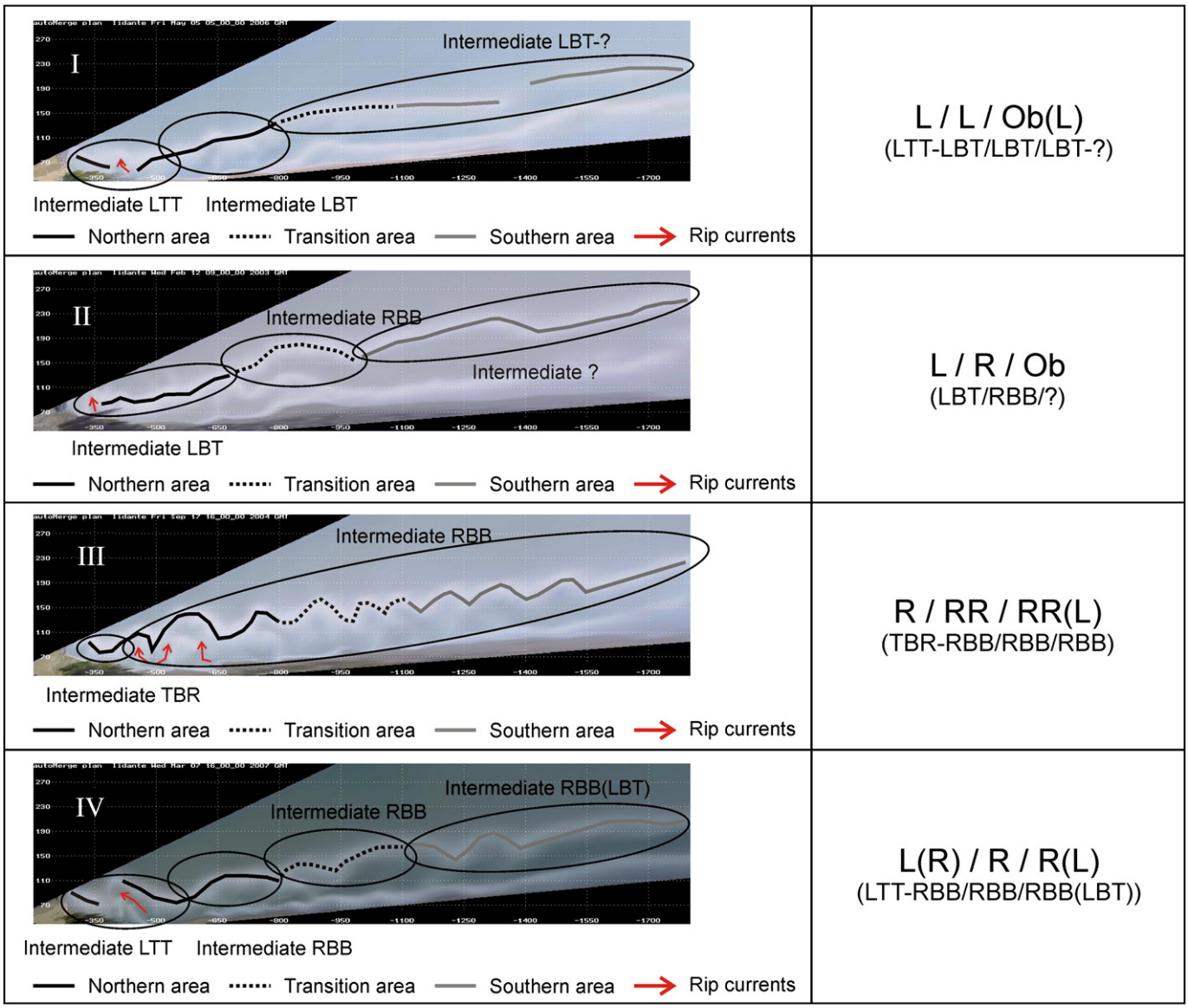

Fig. 6. Four examples of plan views where the white foam band is visible and the correspondent acronyms derived from the visual classification. The correspondence with the Wright and Short (1984) classification for intermediate beach states is indicated. The red arrows show the position of rip currents.

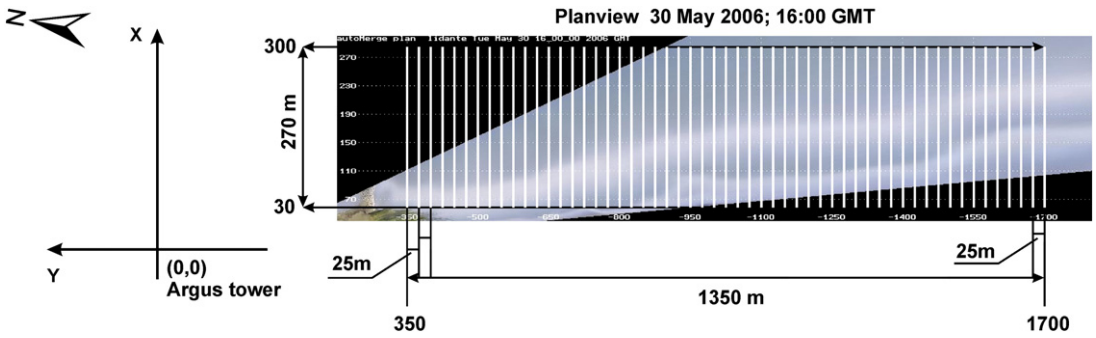

Fig. 7. Scheme of the cross-shore transects spaced at 25 m used to sample the pixel luminosity intensity along the study area. Notice the orientation of the Lido di Dante Argus coordinates system.

but possibly the original French term "en-echelon" better describes them (R. Certain, personal communication).

The comparison between site-specific categorization and the widely used classification of Wright and Short (1984) implies an adaptation of the categories defined by these authors to the case study and to generate new classes if necessary (Lippmann and Holman, 1990; Ranasinghe et al., 2004; Armaroli et al., 2007). An example of four representative morphodynamic classes developed for the site is compared to the traditional approach of Wright and Short (1984) in Fig. 6. In Panel I there is an example of a combination of morphologies characterised by a well-defined Linear Bar (L) that becomes oblique (Ob) with the distance. In Panel II it is possible to see the transition from a linear bar (L) to a crescentic curvilinear bar (R) and then onto two oblique bars (Ob). Panel III shows a configuration of the system with high rhythmicity in most of the studied area (R-RR) except at the southern edge where the bar becomes linear (L) again. Finally, Panel IV is a mixture of all the morphodynamic states described above.

2.3. Pixel luminosity intensity arrays

In the literature there are several methods to identify the bar's crest on Argus images, either working on a grid of pixels or along cross-shore arrays (e.g. see Van Enckevort and Ruessink, 2003a; Van Enckevort et al., 2004). We performed the sampling of the luminosity of pixels along equally spaced cross-shore transects. The transects were located between 350 m and 1700 m from the tower and spaced every 25 m longshore, extending up to 300 m offshore (Fig. 7).

The 25 m spacing was chosen after performing a sensitivity analysis and considering the longshore pixel resolution of the C1 camera. To identify the optimal sampling interval to detect and describe the crescentic forms, the predominant morphodynamic states used for the testing were the rhythmic and the very rhythmic configurations. Different transect spacings were tested (10, 15, 25, and 50 m). The 10 and 15 m interval gave similar results but produced spikes on the plan crest, generating artefacts (e.g. horns and bays that were not in the images). On the contrary, the 50 m spacing was missing some of the forms. Comparing the 10 and the 25 m interval, only 4% of the images used for the sensitivity analysis gave an error in the position of rhythmic forms. It is important to underline that the error was associated with a single horn only in the northern area while the bar crest was generally sampled correctly along the rest of the studied zone. In the end it was decided to use the 25 m sampling because it generated a regular bar crest without artefacts and was able to correctly describe the bar plan crest signal. Moreover, the accuracy in bar location was comparable to the longshore pixel resolution.

2.4. The Longshore Bar Amplitude Identifier Tool

The quantitative analysis of the bar's shape was performed using an Argus automatic tool specifically developed for the site by the authors (L-BAIT, Longshore Bar Amplitude Identifier Tool, Armaroli et al., 2007). The first step was to select the images where the bars were visible, examining breaking wave patterns on time-averaged images. Then quality control was performed on the image's clarity, choosing only data without fog, rain drops on lenses, mist, very heavy wind, etc. This selection is done "by hand" but it is the only time-consuming procedure that has to be performed using the L-BAIT tool. It would be handy to have a tool able to do the selection automatically but there are too many aspects to take into account that can bring the operator to reject an image, such as meteorological factors (e.g. mist), the scarce visibility of foam patterns or the presence of non-continuous foam patterns on the outer bar due to non-breaking waves at certain locations. One good aspect of this visual selection of images is that the operator obtains a detailed overview of all the data available and of what he/she could expect from the automatic analysis. The first procedure is the selection of the images with the hydrodynamic conditions that are suitable for the analysis (described above, low tide between 0 m and −0.2 m and $H_{rms} \leq 1.5$ m). Successively, geometries and plan views of the selected timex are done using standard Argus tools such as the FG (Find Geometry) and AMT (Argus Merge Tool) (Aarninkhof et al., 2003). Then the L-BAIT tool extracts 55 pixel sections from each selected timex. The sections are analysed successively to extract the luminosity peaks. The final output is a matrix for each image with the 55 cross-shore and longshore locations of the bar's plan crest. The run of the tool was sometimes interrupted for quality control procedures to test if the extracted plan crest was correct (direct comparison with timex plan views). The tool offers the possibility to reject one or more peak positions if their location is incorrect. Moreover, to remove the obliquity of the bar plan crest due to the orientation of the Argus system axes, the data are rotated and translated by the tool onto the horizontal axes. The resulting bar plan crest is an oscillatory signal characterised by horns, bays, wave amplitude and wave length. A detailed analysis of wave amplitude and length of the bar crest is not presented in this paper but it will be the subject of a further publication.

2.5. The cross correlation function

To avoid the interpreter uploading every image and defining a morphodynamic class, an automatic comparison is performed by the software using a cross-correlation function (hereafter referred as *x-corr*). The *x-corr* function is an efficient tool to analyze the probability of overlay of two signals, to define whether an unknown function is comparable to a known one and to measure the phase shift between two comparable signals. For the morphodynamic classification the *x-corr* was used to compare plan shapes of the bar.

The bar-signal is not a time-series but a space-series meaning an oscillating signal that varies in space. The oscillations are represented by 3-D submerged features and the space of oscillation coincides with the length of the study area (between the southernmost groyne up to 1700 m southwards). It was decided to compare each "bar-signal" with the one immediately after in time. The conceptual sequence followed for the analysis is: considering 1 to n (B_1; B_2; …; B_{n-1}; B_n) bar-plan-signals, the first step is to visually classify the bar-plan-signal 1 (B_1), that represents the reference morphodynamic state (usually the first in time during the

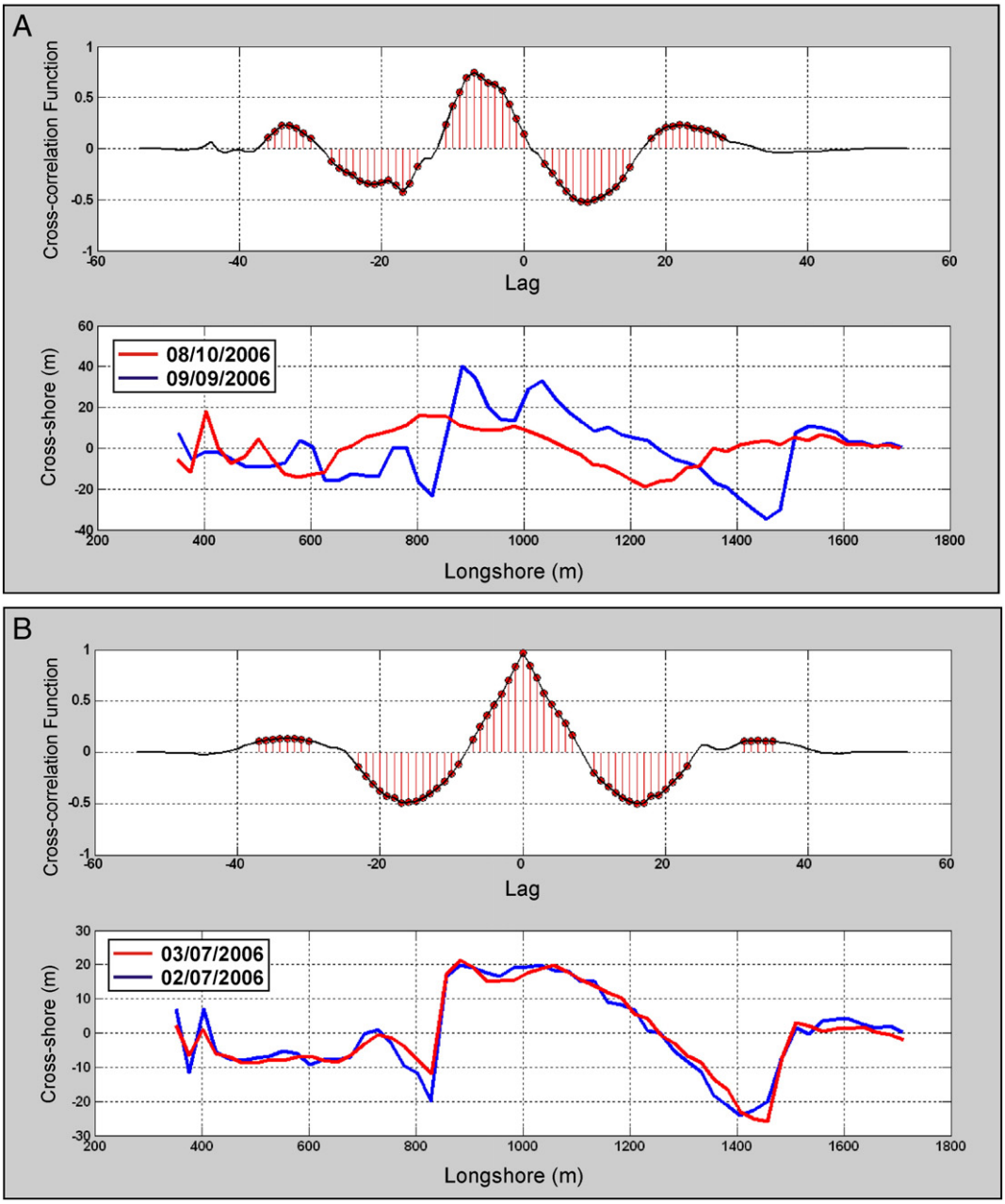

Fig. 8. A: cross-correlation function applied to the bar plan crests of 9 September 2006 and 10 October 2006 showing a non correlation (morphodynamic change); B: cross-correlation function applied to the bar plan crests of 2 and 3 July 2006 showing a strong correlation (no morphodynamic change).

analysed period); then the cross-correlation analysis is applied between the reference signal (B_1) and the one immediately next in time (B_2). If the morphodynamic class of both bars is the same, the procedure continues automatically by considering the non-classified bar (B_2) as the reference morphodynamic class (as it was for B_1). The algorithm then repeats the same steps using the next in time bar-plan-signal (B_3). Ideally, if the morphodynamic state does not change, the procedure goes on automatically until it checks the last relationship between B_{n-1} and B_n without the need for the operator to examine the images and to classify them "by hand". If, instead, the *x-corr* is close to zero, the morphodynamic class is considered changed (see discussion later). Subsequently the operator must visually classify the B_2 bar and must restart the sequence by considering it as the reference morphodynamic state.

To decide which is the *x-corr* value that should be considered as the boundary between "comparable" and "non-comparable" signals, a sensitivity analysis was performed. The bar-plan-shapes for each year between 2003 and 2007 were classified visually and the results were compared with the *x-corr* values obtained automatically. The boundary was chosen as the *x-corr* value that minimises the error between the automatic procedure and the visual classification. This boundary value was found to be 0.72. In fact, a value closer to 1 pre-supposes an almost 100% comparability of the two signals and the procedure fails to put similar bars in the same morphodynamic class. On the contrary, a value closer to 0 puts incomparable signals in the same class. Fig. 8A presents an example of poor correlation between two crests (e.g. morphodynamic change) while Fig. 8B presents two well-correlated crests (same morphodynamic class).

3. Results

3.1. Error analysis in identifying the bar shape

According to the LIDAR survey, in early June 2006 (Fig. 9A), the shape of the offshore bar was generally oblique and almost linear in the central

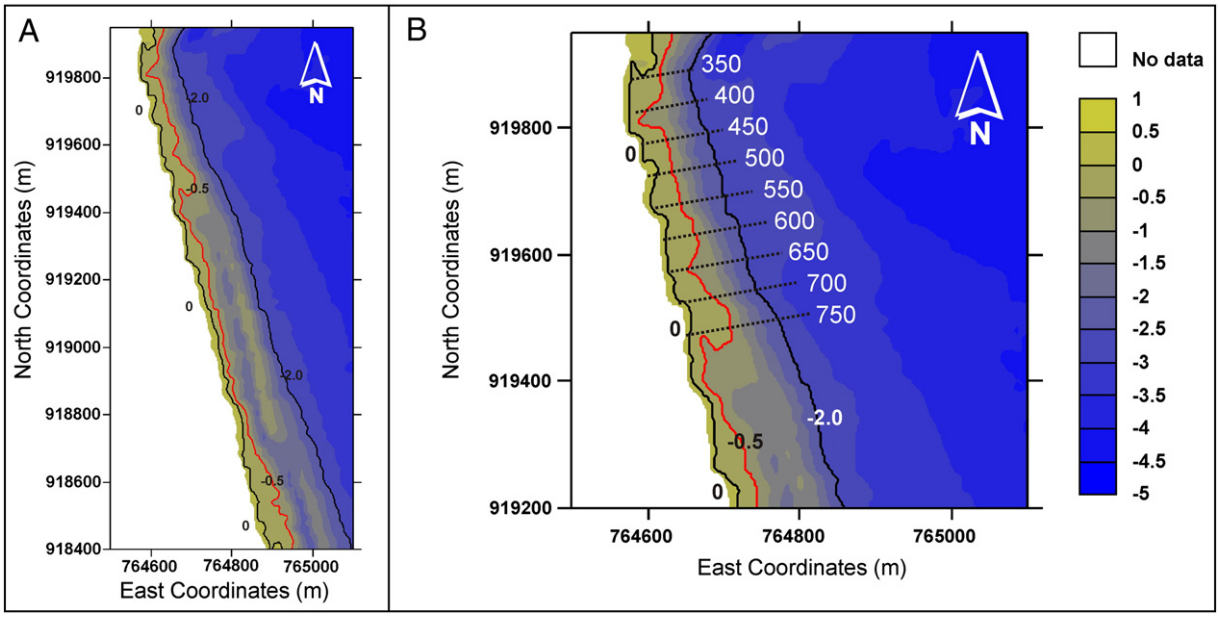

Fig. 9. A: sea floor DTM obtained through Bathymetric LIDAR data (May–June 2006); B: enlargement of the area used for the comparison with image analysis. The transects indicate the positions where pixel arrays were extracted from the images. Elevations are referred to MSL (in meters). Coordinates in UTM 32, Datum ED50.

and southern areas. In the northern area there were intertidal morphologies (ridge and runnel or low tide configuration, intermediate type LTT according to Wright and Short, 1984). The bar crest in direct surveys, as stated above, was defined as the minimum depth between the trough and the bar's seaward foot. Considering the intertidal morphologies in the northern area, the "crest" was chosen as the abrupt change of slope at around low tide (−0.2 m). The comparison was done between the LIDAR data and three Argus bar plan crests extracted from 30 May 2006 and 1–7 June 2006 images. The wave and tide conditions are listed in Table 2 for each day that was studied. Only the images captured at low tide (between 0 m and −0.20 m below MSL) were used to investigate the error associated to the Argus bar plan crest following the methodology described in the previous paragraph (best conditions to see the submerged morphologies, see Armaroli et al. 2006a). The same procedure was followed for the choice of optimal H_{rms} values ($H_{rms} \leq 1.5$ m). The comparison was done along 28 cross-shore profiles spaced every 50 m (Fig. 9B).

A graph with the residuals (LIDAR minus Argus) is shown in Fig. 10A. Between 350 m and 700 m from the tower the trend in the residuals coincides for the three samples, meaning that the crest oscillates similarly in all three, possibly due to the ridge and runnel intertidal bar configuration visible in Fig. 9B. The foam pattern in the northern area is linear, so the video system is not capable of successfully detecting the presence of these intertidal morphologies (e.g. the example of 30 May 2006, Fig. 10B). Between 750 m and 1400 m the residuals do not coincide. Along the 1450 m and 1500 m profiles the error increases up to −20 m. This is the area where there is the gap between the two oblique/almost linear bars (see the image of 1 June in the lowest panel of Fig. 4). Here the bar cross-shore shape is asymmetric and wave breaking occurs on a seaward position with respect to the bar crest (as defined earlier). The last four transects follow the same behaviour defined for the area between 750 m and 1400 m.

Table 2
Waves (H_{rms}) and tide elevation (min/max) for 30th May, 01st June and 07th June 2006.

Waves and tide	30 May 2006	1 June 2006	7 June 2006
H_{rms} (min/max)	0.21 m/1.67 m	0.57 m/1.32 m	0.30 m/0.68 m
Tide (min/max)	−0.31 m/+0.39 m	−0.15 m/+0.20 m	−0.37 m/+0.29 m

For the three tested images (28 samples for each dataset), the mean R^2 value of the linear correlation between LIDAR and Argus bars is 0.995, supporting a very good correspondence between the two types of measurements. The mean RMSE (Root Mean Square Error) of all residuals is 8.3 m. Clearly such a good performance in bar identification is valid for the optimum conditions used for tests. The correlation between observed vs. monitored morphologies is bound to deteriorate as wave height and/or water levels increase.

3.2. Morphodynamic visual and automatic classifications

Using the definitions already shown in Table 1, 27 different "categories" were observed, implying that 27 distinct associations of acronyms could be identified to describe the northern area/central area/southern areas.

The graph in Fig. 11 represent the percentage of appearance of each class, using the number of days in which the class was observed over the total (139 days with visible bars between February 2003 and April 2007). The most frequent categories are the RR/R/RR (14.39%), the RR/R/R(L) (12.95%) and L/Ob(L)/Ob(L) (12.23%). Then the sequence of appearance of the most frequent classes, in descendent order is: L/R/Ob (7.91%) and RR/R/Ob (5.76%). It is important to note that the percentage shown above does not mean that the most frequent class is the more "persistent" in time but that it appears more often in time. Each state is analysed separately because it is visible only when the waves are high enough to break and generate foam patterns on timex images. Except for 2003, when only 25 days were used, in 2004, 2005 and 2006 the number of images is comparable (between 32 and 36 images). In 2007 the number of images available before the nourishment is only 11.

It interesting to note the relationship between the dominance of morphological categories observed at this site and the morphodynamic state predicted by traditional classifications. If the Surf Scaling Parameter (ξ) of Greenspan (1958) is computed using the modal wave conditions at the site ($H_s = 0.5$ m; $T_s = 4.5$ s) and averaging the beach slope (submerged beach = 0.03; intertidal beach = 0.02–0.14), a value around 50 is obtained, that classifies this beach as slightly dissipative in the classification of Wright and Short (1984). In reality, the statistics of occurrence of morphological classes presented in Fig. 11 suggest a dominance of a beach state closer to the intermediate boundary, with

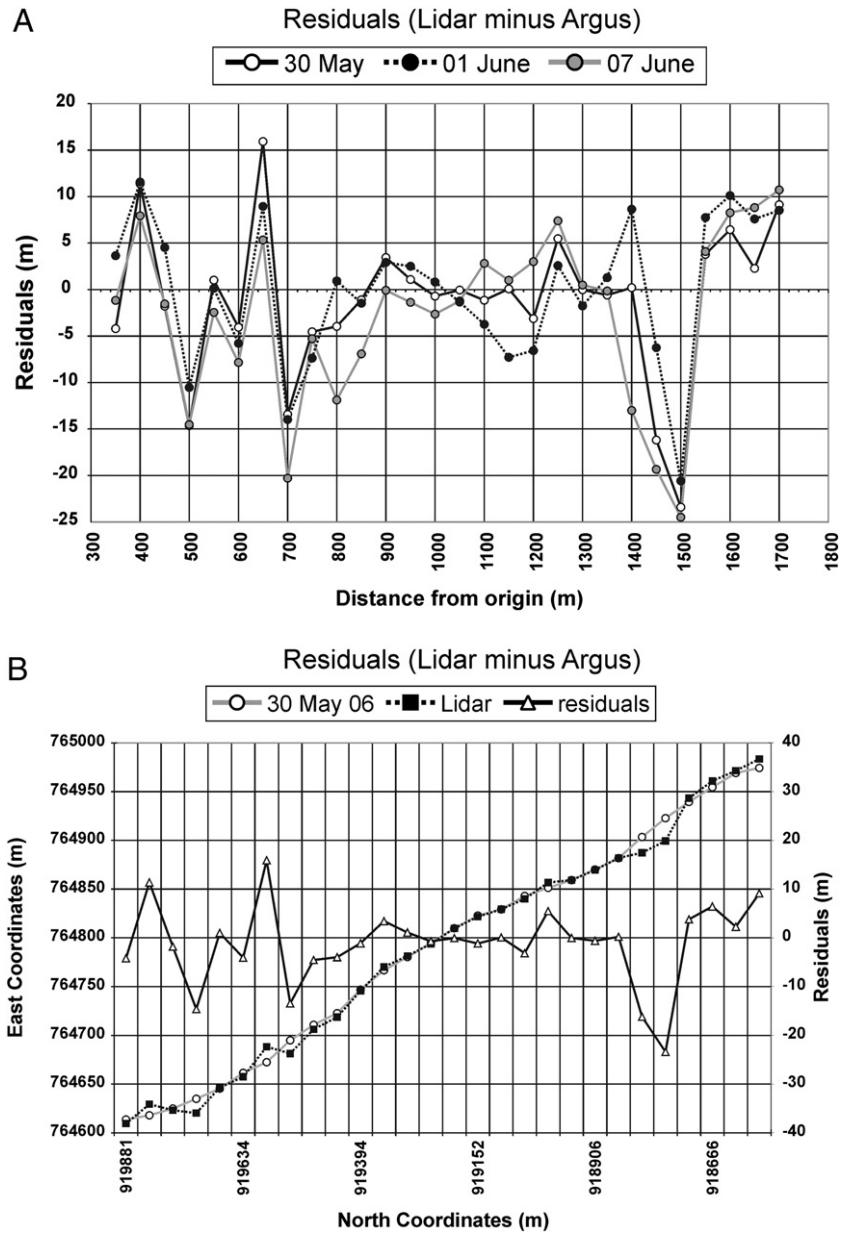

Fig. 10. A: residuals obtained subtracting the cross-shore position of the Argus plan crests sampled on 30 May, 1 June and 7 June 2006 from the LIDAR 2006 bar crest; B: bar plan crests obtained from the LIDAR 2006 and from the 30 May 2006 Argus images. Residuals were obtained subtracting the cross-shore position of the Argus plan crest sampled on 30 May from the LIDAR bar crest.

dominance of the domains RBB–TBR of the classification of Wright and Short (1984). Dean's (Ω) non-dimensional sediment fall velocity (1973) and the Relative Tidal Range (ratio between the Mean Tidal Range and the modal wave height) can instead be used to place this coastline into the Masselink and Short (1993) classification. Using the grain sizes present at the site (submerged beach 2.22 φ; intertidal beach = 2.3–1.1 φ), the values of Ω of 3.21 and RTR of 1.66 predict a dominant intermediate state, with a more or less pronounced single offshore bar and a steep beach face. In reality, the morphology of the longshore bar is well developed, except in the northern part of the area possibly due to the presence of the coastal protection structures.

The observed morphodynamic changes were 4 in 2003, 11 in 2004, 9 in 2005, 10 in 2006 and 3 in 2007. This implies that in 2003 16% of the plan crests show a morphological change; in 2004 the morphodynamic changes were 31% with respect of the total number of comparisons; in 2005 and 2006 were 28% and in 2007 were 27%. The cross-correlation function applied to all planar forms showed a good correspondence with the visual classification. The agreement was 100% in 2003, 72% in 2004, 75% in 2005, 70% in 2006 and 70% in 2007 (mean value 77%).

4. Discussion

4.1. Identification of the point of maximum luminosity on the images

The presence of an error in the identification of the cross-shore position of the bar crest may not only be related to the precision of the method chosen, but also to the cross-shore movement of the breaking zone as waves and tide control wave breaking (Lippmann and Holman, 1989; 1990; Van Enckevort and Ruessink, 2001; Alexander and Holman, 2004). Even if the hydrodynamic conditions are chosen to be the same for the three days used to determine the accuracy of the method, their characteristics were not exactly the same. For example, a slight change in the angle of wave approach to the coast may cause the waves to break at different points even if the longshore bar did not change between images.

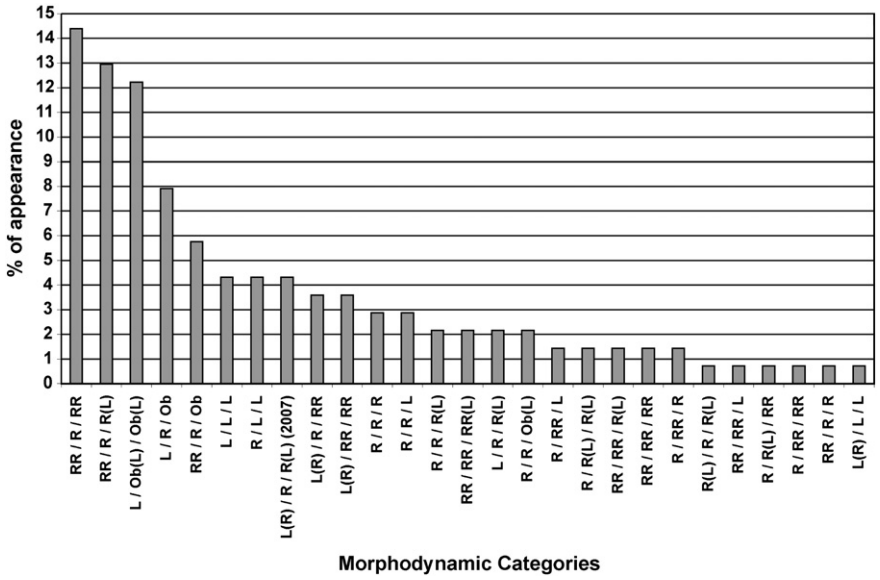

Fig. 11. Percentage of appearance of each observed morphodynamic class out of the total amount of visually classified images (139).

Moreover, the breaking peak itself could be narrow or large in the cross-shore direction, depending on bar shape and wave conditions not only on the analysed day but also on the day/days before, which may have slightly reshaped the bar. According to the comparison between the positions of the bar crest in the video images and the bathymetric surveys, the error is on average 8.3 m, which is the same order of magnitude as that found by Van Enckevort and Ruessink (2001). The good correspondence between our approach and the more rigorous one of the Dutch authors supports the reliability of the dataset discussed in this paper.

Other encouraging evidence of the reliability of the method used is the good correlation between bar positions from the video and bathymetry ($R^2 = 0.995$). Similar studies at Duck (NC, USA) by Plant and Holman (1998) found a correlation which is actually lower ($R^2 = 0.8$) than the present one. As previously explained, this good correlation might be explained by the choice for testing of images captured under "ideal" local wave and tide conditions to see the bar crest. In other conditions, e.g. wide and undefined breaker line, the goodness of the fit may be lower.

The noise found in identifying the bar shape at 750 and 1400 m south of the Argus station is believed to be due not only to the oscillatory form of the bar shape but also to the camera resolution in both the cross-shore and longshore directions. Indeed, the footprint size of the pixels in this area is between 0.5 m and 4 m in the cross-shore and between 8 m and 20 m in the longshore. A further error could be intrinsic to the procedure for extracting the point of maximum luminosity along each section, which is related to the characteristics of the band of foam.

4.2. Changes in the position of the bar crest

The analysis of the crest configuration using the pixel luminosity intensity revealed that the cross-shore mobility of the outer bar was limited to the studied years (2003–2006). A plot of the mean yearly bar position (Fig. 12) proves limited uniform cross-shore movements, while some changes are observed in the spacing and amplitude of the forms. However, some local cross-shore migration can be seen: for example at a longshore distance between 1300 and 1700 m in 2004–2005 the bars are closer to the shoreline than in the other years. Unlike at other Argus sites, a uniform cross-shore landward or seaward migration of the bar in response to wave events was never observed as well as yearly trends which could support a Net Offshore Migration behaviour (otherwise known as NOM, *cf.* Shand, 2007; Ruessink et al., 2009).

Other video-based studies show that the bar can disappear or become attached to the shore like that observed by Van Enckevort and Ruessink (2003a) and Van Enckevort et al. (2004). An offshore migration of the bar in response to storms was also observed by direct surveys at Duck (Lee et al., 1998), while during fair-weather period onshore bar migration was well explained by wave-resolving single-phase modelling (Hsu et al., 2006). Alexander and Holman (2004) confirmed the same tendency using Argus at four different sites with variable wave exposure (Noordwijk, The Netherlands; Agate Beach, Oregon, USA; Duck, North Carolina, USA; and Palm Beach, Australia). It is important to note that this is a typical forced response case, implying a sufficient time duration of the forcing factor (Stive and Reniers, 2003). For a site like Lido di Dante, where the typical duration of the observed storms was 22 h, the process may not be long enough to trigger the offshore migration of the form. On the other hand, in such a context, whenever fair-weather conditions are established, these are characterised by wave height of the order of 0.5 m, which do not break on the offshore bar. However, changes in the bar sinuosity during fair-weather conditions demonstrate that onshore sediment transport exists even under low-energy. The only modification in bar shape is the appearance or disappearance of rhythmic forms, e.g. the passage from to 2-D to 3-D and *vice versa*. The storm of September 2004 (return period of 25 years, see also Ciavola et al., 2007), should have supplied energy to the system to potentially trigger the offshore migration of the bar. However, although the storm of September 2004 had rather high waves (at the peak of the storm $H_s = 5.65$ m), for most of the time (73 h) the waves were between 1.5 and 2 m. A higher wave threshold (e.g. larger than 3 m) was not exceeded for long enough to trigger offshore bar migration. We believe this may be a possible explanation of the limited change in bar position that was observed in the images captured after the event.

There is also the possibility that the NOM model cannot be applied easily in a Mediterranean context. Certain and Barusseau (2005) already discussed in detail this aspect and the reader can find in their paper alternative models to NOM. From a study of a Mediterranean beach at Lido de Sete (France), the authors propose in addition to the NOM behaviour a model of Oscillation around a Position of Equilibrium (OPE) as usual behaviour for the bars, while they suggest that a NOM behaviour is only triggered by extreme storm events (return period 20–50 years). At Lido di Dante, the storm of September 2004 cited above is quite close to the lowest threshold observed in France, and thus may have not been energetic enough to trigger a NOM behaviour.

Finally, there is the possibility that NOM was not observed simply because the life-cycle of these forms at Lido di Dante is longer than the 4 1/2 years of data that were studied. In cases where an onshore bar

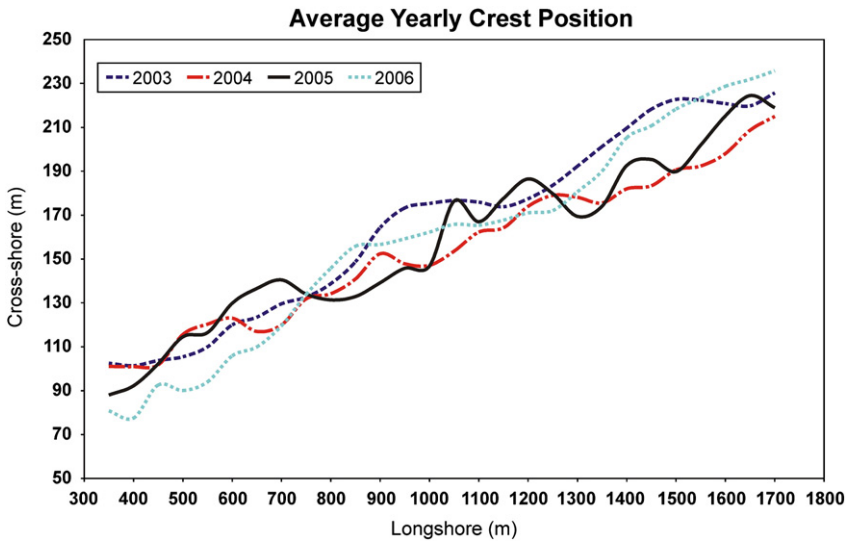

Fig. 12. Mean bar position for each year studied. The position for a given year was obtained averaging all the positions visible on Argus images.

migration was observed, the typical duration of these cycles can span from 1 (Hasaki in Japan, see Kuriyama et al., 2008) to 20 years (Dutch coast, see Ruessink and Kroon, 1994; Wijnberg and Terwindt, 1995). Unfortunately even if the Argus station at the site has been operative up to the present time, the undertaking of the replenishment in 2007 has introduced a perturbation in the system and any natural cycle that may be observed afterwards will have to be discussed in relation to this. Another factor that may explain the absence of interannual cycles is the bar size, which is much smaller than larger systems studied on the Dutch coast by the authors cited above. In a recent paper, Ruessink et al. (2009) came to the conclusion that large bars have a NOM behaviour on an interannual basis, while small bar systems have an episodic NOM in response to the sequence of wave events (e.g. storms). At Lido di Dante not even the second type of behaviour was observed but this may be related to the absence of large storm clusters in the data series.

4.3. Morphodynamic visual classification of the bars

Considering that the only changes observed are essentially related to the appearance and development of three-dimensional forms in the bar, the morphodynamic classification discussed here only deals with the crescentic forms of the bar plan crest.

During the studied period, between February 2003 and September 2007, only 329 images were analysed, representing almost the 2.5% of the total amount of images. This means that the time gap between two observations could be some hours but also a few months. The "residence time" concept proposed by previous authors (Lippmann and Holman, 1990; Ranasinghe et al. 2004) cannot be applied in an easy way to Lido di Dante. In fact, if the morphodynamic state remains the same after several months, one could conclude that this state is stable and that the resident time is the interval between the two observations. In reality this conclusion is incorrect for the site studied here. The bar system is very active and changes its morphodynamic configuration even when there are low energy conditions (Armaroli et al., 2007). This implies that in the period between the two observations, the bar could have changed many times and that only by chance it is the same after a few months when wave conditions are energetic enough to show again the submerged morphologies. In conclusion, what is possible to occasionally see at Lido di Dante is a morphodynamic change, but it is impossible to say exactly when this change occurred.

A topic of study that can also be discussed using the Lido di Dante dataset is the detailed study of the effect of storms on the bar system. Armaroli et al. (2006a) found that a storm with an energy density E (defined as the integer of H_s^2 between the beginning of the storm and its end, after Mendoza and Jimenez, 2006) higher than 500 m^2h is able to straighten the otherwise rhythmic bar, producing a well-defined forced response to changes in wave energy levels. At this point it is very important to underline that the formation of straight bars is not only due to energetic events but there must be other mechanisms involved. In fact, if we consider all the images where the bars are in the linear state (L), we discover that they can become linear after major storms ($E > m^2h$) but they can also remain rhythmic after very energetic events (Fig. 13, 19th to 29 January 2005, clustering of events with waves around 4 m, see Fig. 2). On the contrary, between 25 July and 19 August 2004 during a very calm period (Fig. 13), the bar remains linear (central and southern parts).

From a study of the recent literature that used video-monitoring to understand bar dynamics, the classification is usually done by researchers comparing the bar seen on the Argus imagery (outer, inner and/or intertidal) with traditional morphodynamic classifications (e.g. Wright and Short, 1984) or creating a brand new classification according to the visual observation of oblique or plan view images (e.g. Lippmann and Holman, 1990; Ranasinghe et al., 2004). The relationship between each state is then related to the wave characteristics to find the effect of forcing factors on the bar system. Lippmann and Holman (1990) and Ranasinghe et al. (2004) found that the LBT state (linear bar, Longshore Bar and Trough) is associated with high energy events that are able to straighten the bar, independently from its previous shape. The authors say that the submerged beach continuously shows cycles between different states and that the high-state longshore bar is less persistent than the down-state transitions between "lower" classes (rhythmic bar and beach, RBB; transverse bar and rip, TBR; low tide terrace, LTT). Importantly, the Adriatic Sea generally has a low wave energy, therefore the possibility to see the bars is limited throughout the year. As the study of the plan crest modifications is not done continuously, it not possible to say which are the intermediate configurations between each state and the other one.

The classification proposed here is a "pure" morphological classification because each state is not related to the tide excursion and to wave characteristics. It must be underlined that a statistically significant linear relationship between the forcing factors (e.g. wave characteristics) and the occurrence of each morphodynamic state was investigated but it was not found. This is in agreement with Wijnberg and Kroon (2002) that say "The debate on the mechanisms that cause the transitions between morphologic subtypes is as undecided as that on generation mechanisms, as they tend to be taken as equivalent".

The morphodynamic classification introduced in the current paper is particularly appropriate for sites with rhythmic bars because it is

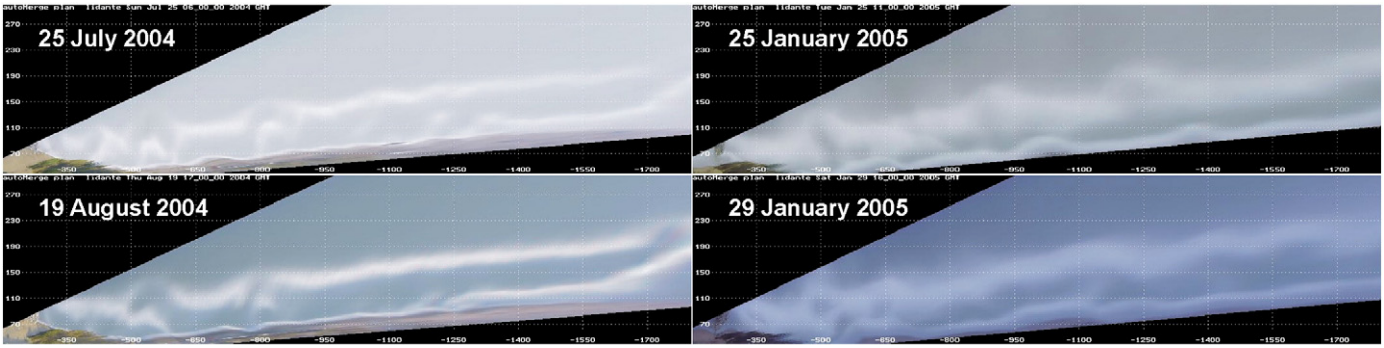

Fig. 13. Left panels: examples of outer linear bars during a very calm period (July–August 2004); Right panels: examples of persistence of outer rhythmic bars after the clustering of three major storms (January 2005). Notice on the 29 January image that the curvature of the forms has decreased.

based on the number of crescentic forms. The observation of all data available shows that the modification of undulated forms is the only change occurring at the site. Clearly this variability can only be detected by image analyses or by very high density bathymetric soundings (e.g. LIDAR).

4.4. Automatic classification of the bars

The efficacy of studying the bar crest using pixel arrays is clear if we consider that the planar outline of the bar can be treated as a signal and several shape analyses can be performed in an automated way. The application of cross-correlation analysis used in this paper seems to be an effective tool for defining the morphological characteristics of one bar signal with respect to the previous one in time.

The agreement between automatic and visual analysis in 2003 was 100%. The predominant morphodynamic state was L/R/Ob (panel II in Fig. 4). The perfect agreement between the visual and the automatic classifications is probably due to the stability of the submerged features that, as described above, show for 84% of the year no changes. These findings are in common between the cross-correlation and the visual classification methods. Between 2004 and 2007 the agreement between the automatic and the visual classification decreases. There are several reasons that could explain this disagreement. The most important is related to the basic principles of the visual classification itself. In fact, the simplified classification presented here involves the counting of rhythmic features along the study area. There are morphological states where "small" crescentic elements are overlaid on a "more significant" crescentic morphology (see an example in Fig. 14, comparison between 8 and 20 October 2006: the two morphodynamic states are different but the *x-corr* considers them as the same morphodynamic state). These small rhythmic forms are developing (Fig. 14, lower figure, red line, between 800 m and 1000 m) but the major crescentic form is still predominant (Fig. 14, lower figure, blue line, between 800 m and 1000 m), breaking down into smaller elements. It was not possible to study which was the time interval necessary for the bar to evolve from one configuration (one crescentic form) to the other (two or more smaller crescentic features) because, for all the reasons described above, the behaviour of the bar cannot be followed in time due to limited wave breaking.

Although in some cases it was possible to visually observe that the rhythmicity was increasing, the *x-corr* function was not able to detect the difference between one bar plan crest and the other because the amplitude of the developing rhythmic elements was too small to be resolved. Another reason that in some cases causes the automatic procedure to fail is the high complexity of the submerged bar. The comparison between complex plan crests that are rhythmic in one part and rhythmic/linear in others sometimes gives a result of no-change between compared images, while in reality the bar has changed. If one looks at the cases when the automatic procedure fails to properly describe the bar, 76% of the time the failure is due to a change in morphodynamic state related to a high complex morphology.

Moreover, the lack of information (images) during fair weather periods after storms does not allow an understanding of the evolution of the submerged beach due to the energetic event. The possibility of sampling the bar crest during a huge storm is limited, as the "ideal" wave condition to sample the crest correctly is $H_{rms} \leq 1.5$ m. This comes from the need to actually see a well-defined white band of foam related to the outer bar. If the waves are higher, the surf zone in the timex images becomes too large to define with confidence the breaking point over the crest.

Another consideration is that the morphological evolution of the Lido di Dante bar system is very dynamic despite the low wave energy generally available for sediment transport. Despite the fact that for most of the year there are low energy wave conditions (76% of the time, as stated above), the bars change frequently, on average for two-thirds of the comparisons undertaken. This means that there must be several mechanisms that are able to move the sand and to generate rhythmic forms, oblique bars and linear bars. Edge waves during storms are a factor normally considered responsible for the formation of crescentics (Bowen and Inman, 1971; Aagaard and Greenwood, 2008) but sometimes bar changes occur when there are low-energy conditions and during summer periods. Using Argus at Egmond in The Netherlands, Van Enckevort et al. (2004) found that during calm periods the bars were able to become rhythmic and very rhythmic, proposing that edge waves are not the only mechanism that is able to explain the formation of 3-D forms. The presence of edge waves during storms was not investigated at Lido di Dante because no equipment was deployed in the breaking zone. On the other hand, from a conceptual viewpoint our video dataset supports the idea that rhythmic forms may develop under low energy conditions. Working on the Israeli coast, which has an energy setting comparable to that of Lido di Dante, Bowman and Goldsmith (1983) reached the conclusion that the formation of the crescentic bars required a short pulse of wave energy (e.g. an H_s between 0.5 and 1.5 m) and from a simple pattern observed 1–2 weeks after a period of higher wave energy, the bars evolved in a more "mature" configuration in 3–7 weeks of extended calm. From our observations it seems that Lido di Dante behaves in a similar manner.

From the application of the automated L-BAIT tool, a comparison of the characteristics of the crescentic bars at Lido di Dante was undertaken with other sites using the relevant literature. This exercise supports future use of our classification but also sets out limits in its applicability. The database is presented in Table 3: the parameters range from physical site characteristics (tide range, nearshore bed slope) to the spacing of the crescentic bars (average wave length). It is important to note that the database does not include all bar datasets present in the literature but only those papers that present all the parameters indicated above. At Lido di Dante the crescentic oscillations were generally spaced about 250 m apart. Looking at the database, sites with comparable wave length are found in Israel, Australia, USA (Duck site).

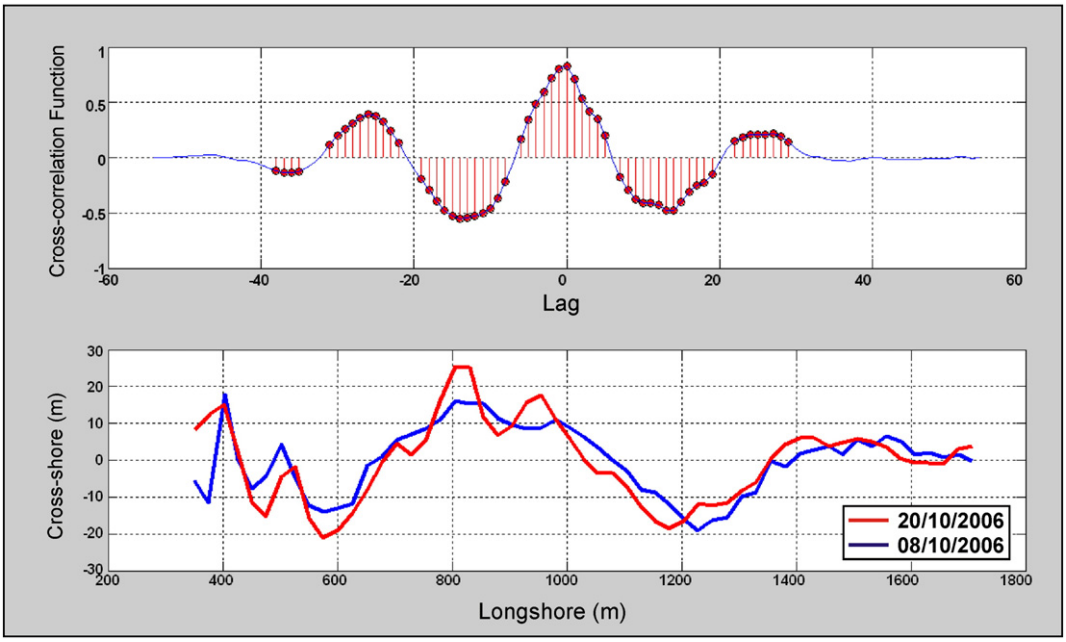

Fig. 14. Cross-correlation function applied between 8 and 20 October 2006. The function value is above the chosen threshold (0.72) but the two plan crests do not belong to the same morphodynamic class as they are visually classified as R/Ob(L)/Ob(L) (8 October 2006) and R/R/Ob(L) (20 October 2006). The error in the automatic procedure is generated by the presence of two "smaller" rhythmic forms (between 800 and 1000 m) that appear where before there was a wider oblique bar.

All these sites have limited tidal ranges (0.5–1.5 m). Out of the sites cited above, the ones in Israel studied by Goldsmith et al. (1982) and Bowman and Goldsmith (1983) show closer resemblance with Lido di Dante and could be studied using the morphodynamics classes presented in this paper.

Possibly self-organization mechanisms influence the bar modification, such as the width of the surf-zone, as numerically explained by Caballeria et al. (2003). Other factors that should be mentioned are the changing water level and water motion due to the tides, the effect of wave groups and low frequency motions in an irregular three-dimensional sea, the time variation of a wave condition, driving for example the migration of rip channel systems (Deigaard et al., 1999). At Lido di Dante no clear pattern in rip occurrence and persistence was observed in the dataset, except for a tendency to occur in what is morphologically defined the "northern" part of the bar system (see Fig. 5), for intermediate morphodynamic states with low to medium rhythmicity. For beach states with elaborated crescentic forms, the spacing of the rips seems irregular across the area. It is noted that studies on sites where a large number of Argus images contain visible rips (e.g. Surfer Paradise, Australia) reach the conclusion that rips may become rapidly topographically controlled soon after a storm event, and their location is then primarily determined by the evolving nearshore morphology rather than hydrodynamic forcing (Turner et al., 2007). Future work on the dataset may address this issue, adopting a rigorous methodology like that of Holman et al. (2006) or Turner et al. (2007).

5. Conclusions

Despite being exposed to generally mild wave conditions, the bar system studied in this paper has shown the capacity of developing

Table 3
Examples of rhythmic bar systems. The lines in bold correspond to sites studies with video monitoring. The dataset is ordered according to year of publication. Except those marked with an asterisk, datasets have been discussed previously by Van Enckevort et al. (2004).

Site	Tidal range (m)	Nearshore bed slope (1/β)	Average spacing of wave forms (m)	Reference
Canada	0.9	200	760	Greenwood and Davidson-Arnott (1975)
Ireland	1.8	100	278	Carter and Kitcher (1979)
Australia	1.5	30	150	Short (1979)
France	0.1	80	340	Barusseau and Saint-Guily (1981)
Israel	0.5	70	265	Goldsmith et al. (1982)
Israel	0.5	100	238	Bowman and Goldsmith (1983)
Duck, NC (USA)	1.2	80	300	Sallengher et al. (1985)
Australia	1.5	50	250	Wright et al. (1986)
NY (USA)	1.1	60	2000	Allen and Psuty (1987)
Duck, NC (USA)	1.2	80	250	Howd and Birkemeier (1987)
Canada	0.0	30	145	Stewart and Davidson-Arnott (1988)
Netherlands	2.0	220	1750	Ruessink (1992)
Netherlands	**1.5**	**120**	**575**	Ruessink et al. (2000)
France (Leucate-Plage)*	0.3	68	600	Certain (2002)
CA (USA)	1.0	100	150	MacMahan et al. (2002)
Netherlands	**1.6**	**150**	**1035**	Van Enckenvort and Ruessink (2003b)
Duck, NC (USA)	**1.1**	**80**	**365**	Van Enckevort et al. (2004)
Miyazaki (Japan)	**1.6**	**80**	**363**	Van Enckevort et al. (2004)
Gold Coast (Australia)	**1.7**	**50**	**483**	Van Enckevort et al. (2004)
Noordwijk (Netherlands)	**1.8**	**150**	**1369**	Van Enckevort et al. (2004)
Italy (Lido di Dante)*	**0.9**	**33**	**256**	Armaroli et al., 2007 and this paper

complex plan shapes of its crest. Using an Argus system installed at the site in February 2003, it was possible to study the submerged beach characteristics and to propose a new simplified morphodynamic classification for rhythmic bar systems. The classification can be applied to other contexts comparable to the current one, e.g. microtidal systems exposed to low wave energy regimes.

Plan views of timex images were visually classified to find the rhythmic characteristics of the bar. The basis of the classification is the quantification of the number of crescentic oscillations that develop along the study area. The choice of the classification criteria derives from the fact that the bar system frequently changed morphodynamic class, but it never changed its cross-shore position becoming attached or detached from the shoreline, disappearing or reforming in a different location.

The initial visual classification of bar morphologies on Argus timex images was evaluated against an automatic procedure developed to compare one bar crest to the next in time, to identify the occurrence of morphodynamic changes. The automatic technique is based on the identification of the breaking point, assuming that it corresponds to the maximum pixel luminosity intensity along equally spaced transects. The longshore interval between arrays was chosen after undertaking a sensitivity analysis that demonstrated how a 25 m spacing was the best compromise between the camera resolution and the necessity to identify most of the rhythmic forms of the crescentic bars. The capability of the procedure to correctly trace the bar crest was calibrated against a LIDAR bathymetric survey, obtaining a Root Mean Square Error of 8.3 m. Then the automatic procedure used cross-correlation to find the similarities between one plan crest and the following one in time. The comparison between the two techniques revealed that the automatic procedure was able to describe the morphodynamic characteristics of the bar system with an agreement with the visual classification that is on average 77% of the cases for the studied years (2003–2007). We think that this level of accuracy is already quite satisfactory, considering the complexity of wave breaking patterns on this bar system. It would be interesting to test on other sites the method used in this paper for mapping bars.

The bars at Lido di Dante were shown to be rhythmic most of the time. They were occasionally rectified after storms but rhythmicity developed again shortly afterwards under mild wave conditions. Unfortunately these mild conditions imply that waves are not breaking over the bar for most of the year, therefore a gap in the sequence of available observations makes it impossible to apply the resident time concept proposed by previous authors.

Acknowledgements

Argus station installation and maintenance at Lido di Dante was partially supported for the years 2002–2005 by the Commission of the European Communities under the FP5-CoastView Project (contract no. EVK-CT-2001-00054). Maintenance thereafter was undertaken by the joint efforts of the authors and R. Archetti (CIRSA-University of Bologna) whom we thank for granting access to the database of recent images. LIDAR data were kindly supplied by ENI. We thank Yann Balouin for help in the collection and processing of survey data. We thank reviewers T. Aagaard and J. Guillén for the constructive comments to the manuscript. This paper is a contribution to the EU-FP7 MICORE Project (contract 202798).

References

Aagaard, T., Greenwood, B., 2008. Infragravity wave contribution to surf zone sediment transport — the role of advection. Mar. Geol. 251, 1–14.
Aarninkhof S.G.J., Kingston K., Morelissen R., 2003. The Argus Runtime Environment, guidelines on installation and use. WL | Delft Hydraulics. Delft, the Netherlands, 53 p.
Alexander, P.S., Holman, R.A., 2004. Quantification of nearshore morphology based on video imaging. Mar. Geol. 208, 101–111.
Allen, J.R., Psuty, N.P., 1987. Morphodynamics of a single barred beach with a rip channel, Fire Island, NY. Proceedings of Coastal Sediments'87, ASCE, pp. 1964–1975.
Archetti, R., 2009. Quantifying the evolution of a beach protected by low crested structures using video monitoring. J. Coast. Res. 25, 884–899.
Armaroli, C., Balouin, Y., Ciavola, P., Capatti, D., 2005. Nearshore bars as a natural protection of beaches, field evidence from Lido di Dante Beach, Adriatic Sea. Proceedings of ICCM'05 Conference, Tavira, Algarve, Portugal, pp. 295–303.
Armaroli, C., Balouin, Y., Ciavola, P., Gardelli, M., 2006a. Bar changes due to storm events using ARGUS: Lido di Dante, Italy. Proceedings of: Coastal Dynamics 2005, ASCE, New York, USA. ISBN: 0-7844-0855-6.
Armaroli, C., Ciavola, P., Balouin, Y., Gatti, M., 2006b. An integrated study of shoreline variability using GIS and ARGUS techniques. J. Coast. Res. SI39, 473–477.
Armaroli, C., Ciavola, P., Caleffi, S., Gardelli, M., 2007. Morphodynamics of nearshore rhythmic forms: an energy-based classification. Proceedings of 2007 International Conference on Coastal Engineering, ASCE, pp. 4009–4021.
Balouin, Y., Ciavola, P., Michel, D., 2006a. Support of subtidal tracer studies to quantify the complex morphodynamics of a river outlet: the Bevano, NE Italy. J. Coast. Res. SI39, 602–607.
Balouin, Y., Ciavola, P., Armaroli, C., 2006b. Sediment transport patterns and coastal evolution at Lido di Dante beach, Adriatic Sea. Proceedings of Coastal Dynamics 2005, ASCE, New York, USA. ISBN: 0-7844-0855-6.
Barusseau, J.P., Saint-Guily, B., 1981. Disposition, caractères et mode de formation des barres d'avant-côtefestonnées du littoral du Languedoc–Roussillon (France). Ocea. Acta. 4, 297–304 (In French with English abstract).
Bowen, A.J., Inman, D.L., 1971. Edge waves and crescentic bars. J. Geophys. Res. 76, 8662–8670.
Bowman, D., Goldsmith, V., 1983. Bar morphology on dissipative beaches: an empirical model. Mar. Geol. 51, 15–33.
Caballeria, M., Coco, G., Falques, A., 2003. Crescentic patterns and self-organization processes on barred beaches. Proceedings of Coastal Sediments 2003, ASCE, New York, USA.
Carter, R.W.G., Kitcher, K.L., 1979. The geomorphology of offshore sand bars on the north coast of Ireland. Proc. R. Irish Ac. Royal Irish Academy, Dublin, Ireland, pp. 1507–1521.
Casadei, C., Drei, E., Lamberti, A., 1998. Evoluzione di un litorale protetto da barriere sommerse: Lido di Dante. Proceedings of XXVI Convegno di Idraulica e di Costruzioni Idrauliche, Catania, Italy, Volume III, pp. 245–256 (in Italian).
Certain R., 2002. Morphodynamique d'une cote sableuse microtidale à barres: le Golfe du Lion (Languedoc–Roussillon). PhD Thesis, Universite de Perpignan, Perpignan, France, 233 p. (in French with English abstract).
Certain, R., Barusseau, J.P., 2005. Conceptual modelling of sand bars morphodynamics for a microtidal beach (Sète, France). Bull. Soc. Géol. Fr. 176, 343–354.
Ciavola, P., Gatti, M., Armaroli, C., Balouin, Y., 2003. Valutazione della variazione della linea di riva nell'area di Lido di Dante (RA) tramite GIS e monitoraggio con DGPS cinematico. Proceedings of Convegni dei Lincei, Roma, Italy, 205, pp. 113–121 (in Italian).
Ciavola, P., Armaroli, C., Chiggiato, J., Valentini, A., Deserti, M., Perini, L., Luciani, P., 2007. Impact of storms along the coastline of Emilia–Romagna: the morphological signature on the Ravenna coastline (Italy). J. Coast. Res. SI50, 540–544.
Coco, G., Ruessink, B.G., Van Eckenvort, I.M.J., Caballeria, M., Falques, A., Holman, R., Plant, N., Turner, I.L., 2004. Video observations of crescentic sand bars and modelling implications. Proceedings of 2004 International Conference of Coastal Engineering, ASCE, pp. 2767–2776.
Davidson, M.A., Van Koningsveld, M., De Kruif, A., Rawson, J., Holman, R.A., Lamberti, A., Medina, R., Kroon, A., Aarninkhof, S.G.J., 2007. The Coastview Project: developing video-derived coastal state indicators in support of coastal zone management. Coastal Eng. 54, 463–475.
Dean, R.G., 1973. Heuristic models of sand transport in the surf zone. Proceedings of First International Australian Engineering Conference, Sydney, Institute of Engineers of Australia, pp. 208–214.
Deigaard, R., Dronen, N., Fredsoe, J., Jensen, J.H., Jorgensen, M.P., 1999. A morphological stability analysis for a long straight barred coast. Coastal Eng. 36, 171–195.
Dolan, R., Hayden, B., 1983. Patterns and prediction of shoreline change. In: Komar, P.D. (Ed.), CRC Handbook of Coastal Processes and Erosion. CRC Press, Boca Raton, USA, pp. 123–149.
Gambolati G., Giunta G., Putti M., Teatini P., Tomasi L., Betti I., Morelli M., Berlamont J., De Backer K., Decouttere C., Monbaliu J., Yu C.S., Broeker I., Kristenser E.D, Elfrink B., Dante A., Gonella M., 1998. Coastal evolution of the Upper Adriatic Sea due to Sea Level Rise, and Natural and Anthropic Land Subsidence. In: CENAS. Kluwer Academic (Ed.), Dordrecht, The Netherlands, pp. 1–34.
Gardelli, M., Caleffi, S., Ciavola, P., 2007. Evoluzione morfodinamica della foce del torrente Bevano. Studi Costieri 13, 55–76 (in Italian with English abstract).
Goldsmith, V., Bowman, D., Kiley, K., 1982. Sequential stage development of crescentic bars: Ha Hoterim Beach, southeastern Mediterranean. J. Sediment. Petrol. 52, 233–249.
Gómez-Pujol, L., Orfila, A., Cañellas, B., Alvarez-Ellacuria, A., Méndez, F.J., Medin, R., Tintoré, J., 2007. Morphodynamic classification of sandy beaches in low energetic marine environment. Mar. Geol. 242, 235–246.
Greenspan, H.P., 1958. On the breaking of water waves of finite amplitude on a sloping beach. J. Fluid Mech. 4, 330–334.
Greenwood, B., Davidson-Arnott, R.G.D., 1975. Marine bars and nearshore sedimentary processes, Kouchibouguac Bay, New Brunswick, Canada. In: Hails, J.R., Carr, A.P. (Eds.), Nearshore Sediments Dynamics and Sedimentation. Wiley-Interscience, New York, USA, pp. 123–150.
Guillén, J., Palanques, A., 1993. Longshore bar and trough systems in a microtidal, storm-wave dominated coast: the Ebro Delta (Northwestern Mediterranean). Mar. Geol. 115, 239–252.
Holland, K.T., Holman, R.A., Lippmann, T.C., Stanley, J., Plant, N., 1997. Practical use of video imagery in nearshore oceanographic field studies. J. Oceanic Eng. 22, 81–92.
Holman, R.A., Stanley, J., 2007. The history and technical capability of Argus. Coastal Eng. 54, 477–491.
Holman, R.A., Symonds, G., Thornton, E.B., Ranasinghe, R., 2006. Rip spacing on an embayed beach. J. Geophys. Res. 111, C01006. doi:10.1029/2005/JC002965 (17p.

Howd, P.A., Birkemeier, W.A., 1987. Storm-induced morphology changes during Duck85. Proceedings of Coastal Sediments'87, ASCE, pp. 834–847.
Hsu, T., Elgar, S., Guza, R.T., 2006. Wave-induced sediment transport and onshore sandbar migration. Coastal Eng. 53, 817–824.
Huntley, D.A., Bowen, A.J., 1975. Comparison of the hydrodynamics of steep and shallow beaches. In: Hails, J.R., Carr, A.P. (Eds.), Nearshore Sediments Dynamics and Sedimentation. Wiley-Interscience, New York, USA, pp. 69–109.
Idroser, 1996. Progetto di piano di difesa del mare e la riqualificazione ambientale del litorale della Regione Emilia–Romagna, relazione generale. Regione Emilia–Romagna, Bologna, Italy, pp. 16–43 (in Italian).
Jiménez, J.A., Guillén, J., Falqués, A., 2008. Comment on the article "Morphodynamic classification of sandy beaches in low energetic marine environment" by Gómez-Pujol L., Orfila A., Cañellas B., Alvarez-Ellacuria A., Méndez F.J. Medina R. Tintoré J. Mar. Geol. 255, 96–101.
Kroon, A., Davidson, M.A., Aarninkhof, S.G.J., Archetti, R., Armaroli, C., Gonzales, M., Medri, S., Osorio, A., Aagaard, T., Holman, R.A., Spanhoff, R., 2007. Application of remote sensing video system for coastline management problems. Coastal Eng. 54, 493–505.
Kuriyama, Y., Ito, Y., Yanagishima, S., 2008. Medium-term variations of bar properties and their linkages with environmental factors at Hasaki, Japan. Mar. Geol. 248, 1–10.
Lee, G., Nicholls, R.J., Birkemeier, W.A., 1998. Storm-driven variability of the beach-nearshore profile at Duck, North Carolina, USA, 1981–1991. Mar. Geol. 148, 163–177.
Lippmann, T.C., Holman, R.A., 1989. Quantification of sand bar morphology: a video technique based on wave dissipation. J. Geophys. Res. 94, 995–1011.
Lippmann, T.C., Holman, R.A., 1990. The spatial and temporal variability of sand bar morphology. J. Geophys. Res. 95, 11575–11590.
MacMahan, J., Reniers, A.J.H.M., Thornton, E.B., Stanton, T., Dean, R.G., 2002. RIPEX: rip current pulsation measurement. Proceedings of 2002 International Conference on Coastal Engineering, ASCE, pp. 736–746.
Masselink, G., Short, A.D., 1993. The effect of tide range on beach morphodynamics. J. Coast. Res. 9, 785–800.
Medellín, G., Medina, R., Falqués, A., González, M., 2008. Coastline sand waves on a low-energy beach at "El Puntal" spit, Spain. Mar. Geol. 250, 143–156.
Mendoza, E.T., Jimenez, J.A., 2006. Factors controlling vulnerability to storm impacts along the Catalonian coast. Proceedings of 2004 International Conference on Coastal Engineering, ASCE, pp. 3087–3099.
Ojeda, E., Guillén, J., 2006. Monitoring beach nourishment based on detailed observations with video measurements. J. Coast. Res. SI48, 100–106.
Ojeda, E., Guillén, J., 2008. Shoreline dynamics and beach rotation of artificial embayed beaches. Mar. Geol. 253, 51–62.
Ojeda, E., Guillén, J., Ribas, F., 2006. Bar and shoreline coupling in artificial embayed beaches. Proceedings of 2004 International Conference of Coastal Engineering, ASCE, pp. 2714–2725.
Ortega-Sánchez, M., Fachin, S., Rancho, F., Losada, M.A., 2008. Relation between beachface morphology and wave climate at Trafalgar Beach (Cádiz, Spain). Geomorphology 99, 171–185.
Plant, N.G., Holman, R.A., 1998. Extracting morphology information from field data. Proceedings of 1998 International Conference of Coastal Engineering, ASCE, pp. 2773–2784.
Ranasinghe, R., Symonds, G., Black, K., Holman, R.A., 2004. Morphodynamics of intermediate beaches: a video imaging and numerical modelling study. Coastal Eng. 51, 629–655.
Ribas, F., Ojeda, E., Price, T.D., Guillén, J., 2010. Assessing the suitability of video imaging for studying the dynamics of nearshore sandbars in tideless beaches. IEEE Trans. Geosci. Remote Sens. 48. doi:10.1109/TGRS.2009.2039576.
Ruessink, B.G., 1992. The nearshore morphology of Terschelling (1965–1991). Rep. R92-11. Institute for Marine and Atmospheric Research, Utrecht, The Netherlands.
Ruessink, B.G., Kroon, A., 1994. The behavior of a multiple bar system in the nearshore zone of Terschelling, The Netherlands: 1965–1993. Mar. Geol. 121, 187–197.
Ruessink, B.G., Van Enckevort, I.M.J., Kingston, K.S., Davidson, M.A., 2000. Analysis of observed two- and three-dimensional nearshore bar behaviour. Mar. Geol. 169, 161–183.
Ruessink, B.G., Pape, L., Turner, I.L., 2009. Daily to interannual cross-shore sand bar migration: observations from a multiple sand bar system. Cont. Shelf Res. 29, 1663–1677.
Sallengher, A.H., Holman, R.A., Birkemeier, W., 1985. Storm-induced response of a nearshore-bar system. Mar. Geol. 64, 237–257.
Shand, R.D., 2007. Bar splitting: system attributes and sediment budget implications for a net offshore migrating bar system. J. Coast. Res. SI50, 721–730.
Short, A.D., 1979. Three dimensional beach-stage model. J. Geol. 87, 553–571.
Short, A.D., 2006. Australian beach systems—nature and distribution. J. Coast. Res. 22, 11–27.
Short, A.D., Aagaard, T., 1993. Single and multi-bar beach change models. J. Coast. Res. SI15, 141–157.
Siegle, E., Huntley, D.A., Davidson, M.A., 2007. Coupling video imaging and numerical modelling for the study of inlet morphodynamics. Mar. Geol. 236, 143–163.
Stewart, C.J., Davidson-Arnott, R.G.D., 1988. Morphology, formation and migration of longshore sandwaves; Long point, Lake Erie, Canada. Mar. Geol. 81, 63–77.
Stive, M.J.F., Reniers, A.J.H.M., 2003. Sandbars in motion. Science 299, 1855–1856.
Teatini, P., Ferronato, M., Gambolati, G., Bertoni, W., Gonella, M., 2005. A century of land subsidence in Ravenna, Italy. Environ. Geol. 47, 831–846.
Turner, I.L., Aarninkhof, S.G.J., Holman, R.A., 2006. Coastal imaging applications and research in Australia. J. Coast. Res. 22, 37–48.
Turner, I.L., Whyte, D., Ruessink, G.B., Ranasinghe, R., 2007. Observations of rip spacing, persistence and mobility at a long, straight coastline. Mar. Geol. 236, 209–221.
Van Enckevort, I.M.J., Ruessink, B.G., 2001. Effect of hydrodynamics and bathymetry of video estimates of nearshore sand bar position. J. Geophys. Res. 106, 16969–16979.
Van Enckevort, I.M.J., Ruessink, B.G., 2003a. Video observations of nearshore bar behaviour. Part 1: alongshore uniform variability. Cont. Shelf Res. 23, 501–512.
Van Enckevort, I.M.J., Ruessink, B.G., 2003b. Video observations of nearshore bar behaviour. Part 2: alongshore non-uniform variability. Cont. Shelf Res. 23, 513–532.
Van Enckevort, I.M.J., Ruessink, B.G., Coco, G., Suzuki, K., Turner, I.L., Plant, N.G., Holman, R.A., 2004. Observation of nearshore crescentic sandbars. J. Geophys. Res. 109. doi:10.1029/2993JC002214.
Wijnberg, K.M., Kroon, A., 2002. Barred beaches. Geomorphology 48, 103–120.
Wijnberg, K.M., Terwindt, J.H.J., 1995. Extracting decadal morphological behaviour from high-resolution, long-term bathymetric surveys along the Holland coast using eigenfunction analysis. Mar. Geol. 126, 301–330.
Wright, L.D., Short, A.D., 1983. Morphodynamics of beaches and surf zones in Australia. In: Komar, P.D. (Ed.), Handbook of Coastal Processes and Erosion. CRC press, Boca Raton, USA, pp. 35–64.
Wright, L.D., Short, A.D., 1984. Morphodynamic variability of surf zones and beaches. Mar. Geol. 56, 93–118.
Wright, L.D., Chappell, J., Thom, B.G., Bradshaw, M.P., Cowell, P.J., 1979. Morphodynamics of reflective and dissipative beach and inshore systems, Southeastern Australia. Mar. Geol. 32, 105–140.
Wright, L.D., Guza, R.T., Short, A.D., 1982a. Dynamics of a high-energy dissipative surf zone. Mar. Geol. 45, 41–62.
Wright, L.D., Nielsen, P., Short, A.D., Green, M.O., 1982b. Morphodynamics of a microtidal beach. Mar. Geol. 50, 97–128.
Wright, L.D., Nielsen, P., Shi, N.C., Short, A.D., 1986. Morphodynamics of a bar-trough surf zone. Mar. Geol. 70, 251–285.